



OPEN ACCESS

EDITED BY

Alessia Remigante,
University of Messina, Italy

REVIEWED BY

Roberta De Zio,
University of Bari Aldo Moro, Italy
Teresa Pasqua,
University Magna Graecia of Catanzaro,
Italy

*CORRESPONDENCE

Roberto Berra-Romani,
rberra001@hotmail.com
Francesco Moccia,
francesco.moccia@unipv.it

SPECIALTY SECTION

This article was submitted to Cellular Biochemistry, a section of the journal Frontiers in Cell and Developmental Biology

RECEIVED 11 July 2022

ACCEPTED 08 August 2022

PUBLISHED 02 September 2022

CITATION

Berra-Romani R, Vargaz-Guadarrama A, Sánchez-Gómez J, Coyotl-Santiago N, Hernández-Arambide E, Avelino-Cruz JE, García-Carrasco M, Savio M, Pellavio G, Laforenza U, Lagunas-Martínez A and Moccia F (2022), Histamine activates an intracellular Ca²⁺ signal in normal human lung fibroblast WI-38 cells. *Front. Cell Dev. Biol.* 10:991659. doi: 10.3389/fcell.2022.991659

COPYRIGHT

© 2022 Berra-Romani, Vargaz-Guadarrama, Sánchez-Gómez, Coyotl-Santiago, Hernández-Arambide, Avelino-Cruz, García-Carrasco, Savio, Pellavio, Laforenza, Lagunas-Martínez and Moccia. This is an open-access article distributed under the terms of the [Creative Commons Attribution License \(CC BY\)](https://creativecommons.org/licenses/by/4.0/). The use, distribution or reproduction in other forums is permitted, provided the original author(s) and the copyright owner(s) are credited and that the original publication in this journal is cited, in accordance with accepted academic practice. No use, distribution or reproduction is permitted which does not comply with these terms.

Histamine activates an intracellular Ca²⁺ signal in normal human lung fibroblast WI-38 cells

Roberto Berra-Romani^{1*}, Ajelet Vargaz-Guadarrama¹, Josué Sánchez-Gómez¹, Nayeli Coyotl-Santiago¹, Efraín Hernández-Arambide¹, José Everardo Avelino-Cruz², Mario García-Carrasco³, Monica Savio⁴, Giorgia Pellavio⁴, Umberto Laforenza⁴, Alfredo Lagunas-Martínez⁵ and Francesco Moccia^{6*}

¹Department of Biomedicine, School of Medicine, Benemérita Universidad Autónoma de Puebla, Puebla, México, ²Laboratory of Molecular Cardiology, Institute of Physiology, Benemérita Universidad Autónoma de Puebla, Puebla, México, ³Department of Immunology, School of Medicine, Benemérita Universidad Autónoma de Puebla, Puebla, México, ⁴Department of Molecular Medicine, University of Pavia, Pavia, Italy, ⁵Direction of Chronic Infections and Cancer, Research Center in Infection Diseases, National Institute of Public Health, Morelos, México, ⁶Laboratory of General Physiology, Department of Biology and Biotechnology "Lazzaro Spallanzani", University of Pavia, Pavia, Italy

Histamine is an inflammatory mediator that can be released from mast cells to induce airway remodeling and cause persistent airflow limitation in asthma. In addition to stimulating airway smooth muscle cell constriction and hyperplasia, histamine promotes pulmonary remodeling by inducing fibroblast proliferation, contraction, and migration. It has long been known that histamine receptor 1 (H1R) mediates the effects of histamine on human pulmonary fibroblasts through an increase in intracellular Ca²⁺ concentration ([Ca²⁺]_i), but the underlying signaling mechanisms are still unknown. Herein, we exploited single-cell Ca²⁺ imaging to assess the signal transduction pathways whereby histamine generates intracellular Ca²⁺ signals in the human fetal lung fibroblast cell line, WI-38. WI-38 fibroblasts were loaded with the Ca²⁺-sensitive fluorophore, FURA-2/AM, and challenged with histamine in the absence and presence of specific pharmacological inhibitors to dissect the Ca²⁺ release/entry pathways responsible for the onset of the Ca²⁺ response. Histamine elicited complex intracellular Ca²⁺ signatures in WI-38 fibroblasts throughout a concentration range spanning between 1 μM and 1 mM. In accord, the Ca²⁺ response to histamine adopted four main temporal patterns, which were, respectively, termed peak, peak-oscillations, peak-plateau-oscillations, and peak-plateau. Histamine-evoked intracellular Ca²⁺ signals were abolished by pyrilamine, which selectively blocks H1R, and significantly reduced by ranitidine, which selectively inhibits H2R. Conversely, the pharmacological blockade of H3R and H4R did not affect the complex increase in [Ca²⁺]_i evoked by histamine in WI-38 fibroblasts. In agreement with these findings, histamine-induced intracellular Ca²⁺ signals were initiated by intracellular Ca²⁺ release from the endoplasmic reticulum through inositol-1,4,5-trisphosphate (InsP₃) receptors (InsP₃R) and sustained by store-operated Ca²⁺ channels (SOCs). Conversely,

L-type voltage-operated Ca^{2+} channels did not support histamine-induced extracellular Ca^{2+} entry. A preliminary transcriptomic analysis confirmed that WI-38 human lung fibroblasts express all the three InsP_3R isoforms as well as STIM2 and Orai3 , which represent the molecular components of SOCs. The pharmacological blockade of InsP_3 and SOC, therefore, could represent an alternative strategy to prevent the pernicious effects of histamine on lung fibroblasts in asthmatic patients.

KEYWORDS

histamine, intracellular Ca^{2+} , lung fibroblasts, WI-38, Ca^{2+} oscillations, InsP_3 receptors, store-operated Ca^{2+} entry

Introduction

Asthma is a heterogeneous disease, generally characterized by chronic inflammation of the airways, defined by a clinical history of respiratory symptoms, such as wheezing, shortness of breath, chest tightness, and cough that vary in intensity and frequency, along with variable expiratory airflow (GBD Diseases and Injuries Collaborators, 2020). About 300 million people suffer from asthma worldwide and it is likely that, by 2025, another 100 million people will be affected by this disease (Dharmage et al., 2019).

The complex network of inflammatory responses in the pathophysiology of asthma involves the release of inflammatory mediators, such as cytokines, chemokines, proteases, and histamine (Murdoch and Lloyd, 2010). Histamine has been a widely recognized inflammatory mediator released from mast cells and could play a key role in the pathophysiology of asthma (Yamauchi and Ogasawara, 2019). Tomioka et al. (1984) estimated that the number of mast cells and the concentration of histamine in bronchoalveolar lavage fluid of asthmatic patients was higher than that of healthy subjects. In addition, Carroll et al. (2002) demonstrated that mast cell degranulation is related to the severity of asthma. Salomonsson et al. (2019) recently reported that elevated levels of circulating mast cell progenitors are related to reduced lung function in asthmatic patients.

In vitro studies demonstrated that histamine stimulated lung fibroblast collagen synthesis (Garbuzenko et al., 2004; Veerappan et al., 2013), migration (Kohyama et al., 2010), proliferation (Jordana et al., 1988; Veerappan et al., 2013) and human lung myofibroblast contraction (Horie et al., 2014). However, the transduction mechanisms whereby histamine leads to these effects in lung fibroblasts are still unclear. Histamine is thought to act by stimulating one or more of four types of plasmalemmal histaminergic receptor (HR) (H1R, H2R, H3R, and H4R) (Panula et al., 2015; Panula, 2021). The expression of H1R and, in less proportion, H2R has been reported in normal human lung fibroblasts (Veerappan et al., 2013) and their participation in promoting lung fibroblast activation has been proposed (Jordana et al., 1988; Garbuzenko et al., 2004;

Kunzmann et al., 2007; Veerappan et al., 2013). In addition, H4R could promote lung fibroblast migration (Kohyama et al., 2010). Stimulation of H1R results in an increase in intracellular Ca^{2+} concentration ($[\text{Ca}^{2+}]_i$) in human valvular myofibroblasts (Liang et al., 2003), pterygial derived fibroblasts (Maini et al., 2002), human gingival fibroblasts (Niisato et al., 1996; Ogata et al., 1999; Gutiérrez-Venegas and Rodríguez-Pérez, 2012), rheumatoid synovial fibroblasts (Zenmyo et al., 1995) human skin fibroblasts (Johnson et al., 1990), human subcutaneous fibroblasts (Pinheiro et al., 2013), and human lung fibroblasts (Zheng et al., 1994; Horie et al., 2014). While H3R are predominantly located in neurons (Abdulrazzaq et al., 2022), H4R are preferentially expressed in cells of the immune system and in blood forming organs, especially in mast cells, dendritic cells, basophils, eosinophils, monocytes, and T lymphocytes (Sarasola et al., 2021). However, immunostaining demonstrated that also human dermal fibroblasts express the H4R (Ikawa et al., 2008). Signaling mechanisms for the H4R receptor are much less well understood but appear to involve an increase in $[\text{Ca}^{2+}]_i$ (Panula et al., 2015).

An elevation in $[\text{Ca}^{2+}]_i$ in fibroblasts is key to protein synthesis, transcription factor activation, migration, progression through the cell cycle, and cell viability (Janssen et al., 2015). Resting $[\text{Ca}^{2+}]_i$ is maintained at very low levels (~100–200 nM), while the extracellular Ca^{2+} concentration is 1000-fold higher (> 1 mM) and the Ca^{2+} concentration in the primary intracellular Ca^{2+} store, the endoplasmic reticulum (ER), fluctuates between 100–800 μM (Sadras et al., 2021a). An array of agonists, such as bradykinin, thrombin, trypsin, adenosine trisphosphate, angiotensin II, and histamine, increases the $[\text{Ca}^{2+}]_i$ in pulmonary fibroblasts at concentrations ranging from approximately 100 nM to 0.1 mM (Janssen et al., 2015). The $[\text{Ca}^{2+}]_i$ can be increased by two main mechanisms upon cellular stimulation: the first one is through the release of Ca^{2+} from the ER and the second one is through the inflow of Ca^{2+} from the extracellular medium. In several cell types, histamine binds to the G_q -protein-coupled receptor (G_qPCR), H1R, which activates phospholipase C (PLC). PLC hydrolyzes a membrane phospholipid, phosphatidylinositol 4, 5 bisphosphate (PIP_2), to produce inositol-1, 4, 5-trisphosphate (InsP_3). InsP_3 triggers Ca^{2+} mobilization from the ER through InsP_3 receptors (InsP_3R) that

are located on the ER membrane and can in turn activate adjacent ryanodine receptors (RyR) through the process of Ca^{2+} -induced Ca^{2+} release (CICR) (Paltauf-Doburzynska et al., 2000; Clapham, 2007; Horie et al., 2014; Ishida et al., 2014; Berra-Romani et al., 2020). Extracellular Ca^{2+} can permeate the plasma membrane through a wide variety of ion channels, including voltage-operated channels (VOC) (Janssen et al., 2015; Rahman et al., 2016) and agonist-operated channels, which comprise three types of channels: 1) receptor-operated channels (ROC) (Saliba et al., 2015), which are ionotropic receptors stimulated by direct ligand binding, 2) second messenger-operated channels (SMOC), which are activated by intracellularly generated mediators, such as cyclic nucleotides, diacylglycerol (Hofmann et al., 2017), and arachidonic acid, and 3) store-operated Ca^{2+} channels (SOC), which are the main Ca^{2+} entry pathway in non-excitable cells. In the ER, Stromal Interaction Molecules (STIM1/2) act as sensors of ER Ca^{2+} concentration that, after a reduction in intraluminal Ca^{2+} , multimerize and translocate towards peripheral ER cisternae to functionally interact with the Ca^{2+} permeable Orai channels on the plasma membrane (Bendiks et al., 2020). The following influx of Ca^{2+} has been termed store-operated Ca^{2+} entry (SOCE) and mediates agonist-induced Ca^{2+} influx in human fibroblasts isolated from several tissues, including lungs (Guzmán-Silva et al., 2015; Vazquez-de-Lara et al., 2018).

It has been demonstrated that histamine triggers an increase in $[\text{Ca}^{2+}]_i$ also in human lung fibroblasts (Zheng et al., 1994; Horie et al., 2014). However, the molecular mechanisms implicated in this response, which are likely to regulate the multiple fibroblast function involved in asthma remodeling, remain to be elucidated. Therefore, this study aimed to examine for the first time the mechanisms underlying histamine-induced increase in $[\text{Ca}^{2+}]_i$ in fetal human pulmonary WI-38 fibroblasts.

Materials and methods

Cell culture

Human fetal lung fibroblast cell lines were purchased from American Type Culture Collection, Collection WI-38 (ATCC[®] CCL-75[™]) and cultured to 75% confluence in DMEM (Dulbecco's Modified Eagle Medium) culture medium supplemented with 10% fetal bovine serum and 1% penicillin-streptomycin at 37°C in an atmosphere of 95% O_2 and 5% CO_2 . Fibroblasts from passages 5–10 were seeded on coverslips for 24 h and then incubated for 48 h in medium devoid of serum.

Physiological solutions

Physiological saline solution (PSS) with the following composition (in mM) 150 NaCl, 6 KCl, 1.5 CaCl_2 1 MgCl_2 ,

10 glucose, 10 HEPES was used for this study. To obtain Ca^{2+} -free physiological saline solution (0Ca^{2+}), Ca^{2+} was replaced with 2 mM NaCl and 0.5 mM EGTA was added as a Ca^{2+} chelator. Osmolarity was measured with an osmometer (Wescor 5500, Logan, UT, United States) solutions were adjusted to pH 7.4 with NaOH.

Measurement of $[\text{Ca}^{2+}]_i$

The technique for Ca^{2+} measurement in fibroblasts has been previously described (Guzmán-Silva et al., 2015), and is explained in detail below. Fibroblasts attached to coverslips were washed twice PSS and incubated with 3 μM FURA-2 acetoxyethyl ester (FURA-2/AM) in PSS for 30 min at room temperature (21°C–23°C). Cells were incubated for 30 min in PSS free of FURA-2/AM. The coverslips were washed and fixed to the bottom of a Petri dish using a drop of silicone. The Petri dish was mounted on a stage of the Axiolab upright epifluorescence microscope (Carl Zeiss, Oberkochen, Germany), equipped with a 100 W mercury lamp (OSRAM HBO 50). A Zeiss X63 Achromplan objective (water immersion, working distance 2.0 mm, numerical aperture 0.9) was used to visualize fibroblasts. Cells were alternately excited at 340 nm and 380 nm using a filter spinning wheel with a shutter (Lambda 10, Sutter Instrument, Novato, CA, United States) and light emitted was detected at 510 nm. The Ca^{2+} signal was measured in individual fibroblasts, using software that allows to delimit each cell by drawing on the acquired images a region of interest. To control the camera (Extended-ISIS camera, Photonic Science, Millham, United Kingdom), the filter rotating wheel, as well as to draw the regions of interest of the fluorescent signal to be measured, a customized software, previously validated, running in LINUX environment, was used. The signal measurement was captured every 3 s and the images obtained were stored on a hard disk and subsequently converted into 340/380 ratio images using ImageJ software (National Institutes of Health, United States, <https://imagej.nih.gov/ij/>). An increase in 340/380 is indicative of an elevation in $[\text{Ca}^{2+}]_i$ (Ferrera et al., 2021; Remigante et al., 2021). Experiments were performed at room temperature (21°C–23°C). All experiments were performed in triplicate using 3 different passages of fibroblasts for each of the conditions.

RT-qPCR

Total RNA was isolated from fibroblasts using QIAzol Lysis Reagent (Qiagen SpA, Milan, Italy), and reverse transcription was performed as described in (Ferrera et al., 2021; Negri et al., 2021). Reverse transcription was always performed in the presence (positive) or in the absence (negative control) of the reverse transcriptase enzyme (not shown), as shown elsewhere

TABLE 1 Primer sequences used for reverse transcription/polymerase chain reaction.

Gene	Primer sequences	Size (bp)	Accession number	
Orai1	Forward-5'-AGTTACTCCGAGGTGATGAG-3'	257	NM_032790.3	
	Reverse-5'-ATGCAGGTGCTGATCATGAG-3'			
Orai2	Forward-5'-CCATAAGGGCATGGATTACC-3'	334	NM_001126340.1	variant 1
	Reverse-5'-CAGGTTGTGGATGTTGCTCA-3'		NM_032831.2	variant 2
Orai3	Forward-5'-CCAAGCTCAAAGCTTCCAGCC-3'	159	NM_152,288.2	
	Reverse-5'-CAAAGAGGTGCACAGCCACCA-3'			
Stim1	Forward-5'-CCTCAGTATGAGGAGACCTT-3'	347	NM_003156.3	
	Reverse-5'-TCCTGAAGGTCATGCAGACT-3'			
Stim2	Forward-5'-AAACACAGCCATCTGCACAG-3'	186	NM_020860.2	
	Reverse-5'-GGGAAGTGTCTGTTCTTTTGA -3'			
InsP ₃ R1	Forward 5'-TCAACAAACTGCACCACGCT-3'	180	ENSG00000150995	
	Reverse 5'-CTCTCATGGCATTCTTCTCC-3'			
InsP ₃ R2	Forward 5'-ACCTTGGG GTTAGTGGATGA-3'	158	ENSG00000123104	
	Reverse 5'-CCTTGTTTGGCTTGCTTTGC-3'			
InsP ₃ R3	Forward 5'-TGGCTTCATCAGCACTTTGG-3'	173	ENSG00000096433	
	Reverse 5'-TGTCTGCTTAGTCTGCTTG-3'			
RyR1	Hs00166991 Thermo Fisher Scientific	75	NM_000540.3	
RyR2	Hs00181461 Thermo Fisher Scientific	65	NM_001035	
RyR3	Hs00168821 Thermo Fisher Scientific	63	NM_001036.6	
Trpc1	Forward 5'-ATCCTACACTGGTGGCAGAA-3'	307		
	Reverse 5'-AACAAAGCAAAGCAGGTGCC-3'			
Trpc3	Forward 5'-GGAGATCTGGAATCAGCAGA-3'	336	NM_001130698.1	v
	Reverse 5'-AAGCAGACCCAGGAAGATGA-3'		NM_003305.2	variant
Trpc4	Forward 5'-ACCTGGGACCTCTGCAAATA-3' Reverse 5'-ACATGGTGGCACCAACAAAC-3'	300	NM_016179.2	va
			NM_001135955.1	va
			NM_001135956.1	v
			NM_001135957.1	va
			NM_003306.1	va
			NM_001135958.1	va
			NM_012471.2	
			NM_004621.5	
Trpc5	Forward 5'-GAGATGACCACAGTGAAGAG-3'	221	NM_012471.2	
	Reverse 5'-AGACAGCATGGGAAACAGGA-3'			
Trpc6	Forward 5'-AGCTGTTCCAGGCCATAAA-3'	341	NM_004621.5	
	Reverse 5'-AAGGAGTTCATAGCGGAGAC-3'			
Trpc7	Forward 5'-CACTTGTGGAACCTGTAGA-3'	387	NM_020389.1	
	Reverse 5'-CATCCAATCATGAAGGCCA-3'			

(Zuccolo et al., 2019; Zuccolini et al., 2022). cDNA amplification was performed using KAPA SYBR FAST qPCR Master Mix (KAPA BIOSYSTEMS, United States), and the primers used for amplification are listed in Table 1. The conditions were as follows: initial denaturation at 95°C for 5 min; 40 cycles of denaturation at 95°C for 10 s; annealing and extension at 60°C for 30 s, PCR products were separated on a 3% Nusieve[®] (2:1) gel agarose, stained with ethidium bromide, and acquired with the iBright™ CL1000 Imaging System (Thermo Fisher Scientific Inc., United States). The molecular weight of the PCR products was compared with the DNA molecular weight marker VIII (Roche Molecular Biochemicals, Italy).

Data analysis

For the acquisition of fluorescence values, ImageJ software was used, and Origin Pro 2021 and GraphPad Prism 8.0 were used for graphing and statistical analysis of the results.

Statistical design

Data were expressed as mean ± standard error (SE). Non-Gaussian data, identified by the D'Agostino and Pearson omnibus normality test ($p \leq 0.05$) were statistically analyzed by the nonparametric Mann-

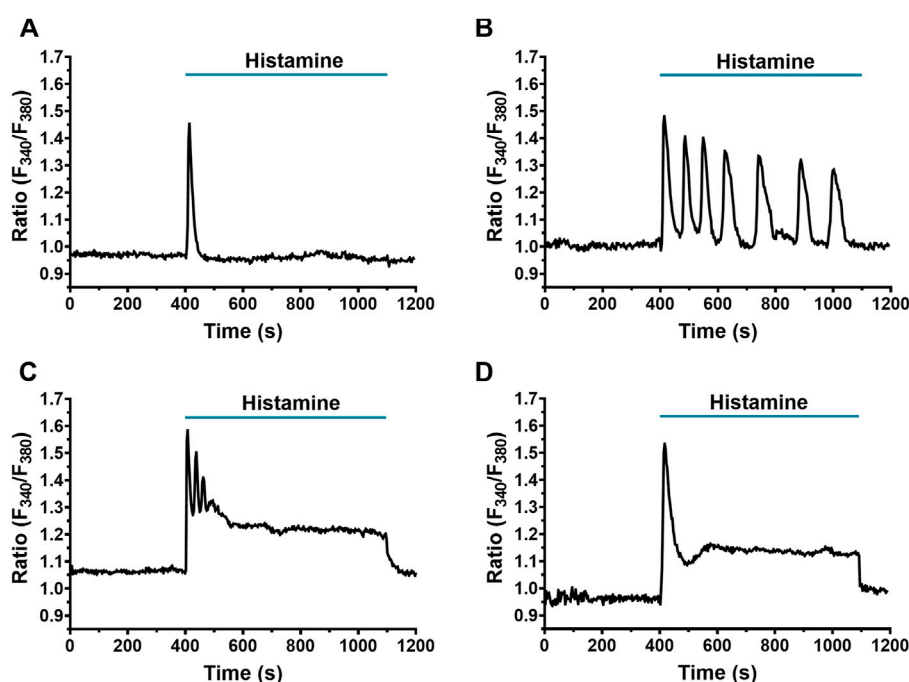


FIGURE 1

Heterogeneity in the Ca^{2+} response elicited by histamine in WI-38 human lung fibroblasts. Application of histamine ($300 \mu\text{M}$) elicited different Ca^{2+} signal patterns in FURA-2 AM-loaded WI-38 human lung fibroblasts. The intracellular Ca^{2+} signal consisted of (A) a rapid Ca^{2+} peak (spike) (19.28% of cells analyzed) which could be followed by (B) Ca^{2+} oscillations (64.70%) (peak-oscillations), (C) sustained plateau, superimposed by Ca^{2+} oscillations (13.39%) (peak-plateau-oscillations) or (D) only a plateau (0.65%) (peak-plateau). In this and the following figures, histamine was added at the time indicated by the horizontal bar drawn over the Ca^{2+} signal recording.

Whitney test for two groups and Kruskal–Wallis for more than two groups. For normal data, an unpaired Student *t*-test for two groups and ANOVA for more than two groups were used. A value of $p \leq 0.05$ was considered statistically significant.

Histamine concentration-response data were adjusted by the following Eq. 1:

$$Y = \frac{100}{1 + \frac{EC_{50}}{[\text{Histamine}]}} \quad (1)$$

where *Y* is the response (relative to the Ca^{2+} transient amplitude), [Histamine] is the histamine concentration and the mean maximal effective concentration (EC_{50}) is the [Histamine] that induced 50% of the maximal response.

Results

Histamine causes a heterogeneous Ca^{2+} signal in human lung fibroblasts of the WI-38 cell line

Using digital fluorescence imaging with FURA-2/AM [Ca^{2+}]_i was measured simultaneously in several individual fibroblasts from the same population. A 22.5% of WI-38 fibroblasts displayed spontaneous

Ca^{2+} oscillations, as also reported in human cardiac fibroblasts (Chen et al., 2010). These cells were, therefore, discarded from subsequent analysis (Faris et al., 2022). Application of histamine ($300 \mu\text{M}$), even in cells in the same microscopic field, elicited Ca^{2+} signals showing heterogeneous kinetics, which were classified into 4 different patterns: the first consisted of a rapid and transient increase in [Ca^{2+}]_i, termed peak (59/306 cells, 19.28%, Figure 1A); the second in a peak followed by cyclic increases and decreases in [Ca^{2+}]_i, termed peak-oscillations (198/306 cells, 64.70%, Figure 1B); the third in a peak with oscillations and a sustained increase in [Ca^{2+}]_i, termed peak-plateau-oscillations (41/306 cells, 13.39%, Figure 1C); and finally, the fourth pattern which was the least frequent, consisted of a peak accompanied by a plateau, and was termed peak-plateau (2/306 cells, 0.65%, Figure 1D). Only 1.96% (6/306 cells) of the analyzed fibroblasts did not respond to histamine $300 \mu\text{M}$.

Histamine generates a Ca^{2+} signal in a concentration-dependent manner in WI-38 human lung fibroblasts

Typical recordings of the Ca^{2+} signals evoked by different histamine concentrations (100 nM–1 mM) are shown in Figure 2A. Histamine did not elicit any discernible increase in

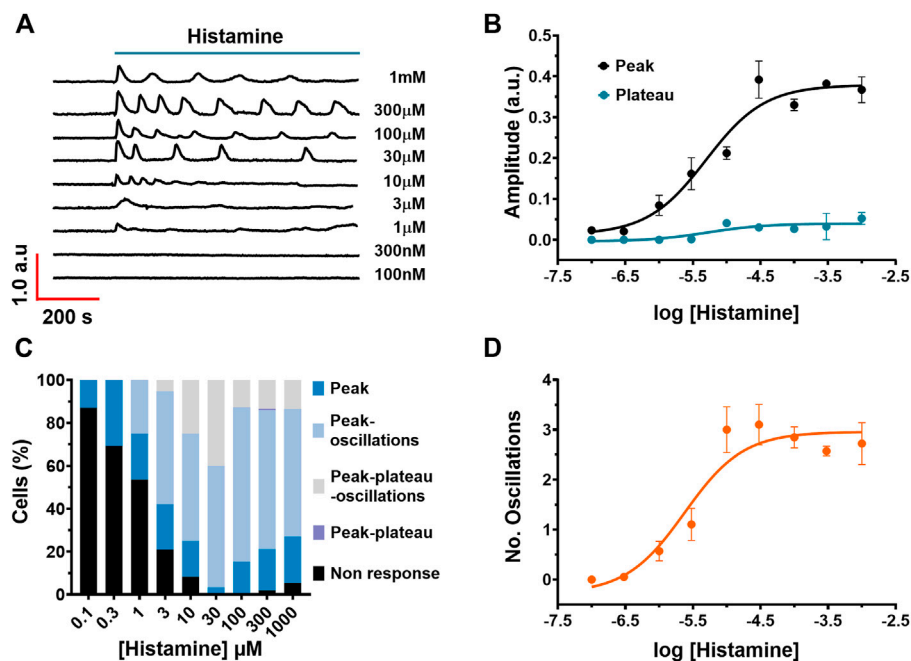


FIGURE 2

Concentration-dependent effect of histamine on Ca^{2+} signalling in WI-38 human lung fibroblasts. (A) Typical intracellular Ca^{2+} recordings in WI-38 cells loaded with FURA-2/AM exposed to different histamine concentrations ranging from 100 nM to 1 mM. The baseline of Ca^{2+} tracings has been shifted to avoid their overlapping for representation purposes. (B) Non-cumulative concentration-response relationship. Data points are the mean \pm SE of the initial Ca^{2+} peak amplitude (black circles) or plateau amplitude (blue circles) plotted against the logarithm of histamine concentration. The continuous curves were obtained by fitting the data to Eq. 1, as shown in Materials and methods, which yielded EC_{50} values of 4.96 and 5.25 μM for peak amplitude (black line) and plateau amplitude (blue line), respectively. Data points were obtained of at least 19 cells. (C) Percentage of cells that presented each of the Ca^{2+} response patterns indicated in function of histamine concentrations applied to WI-38 fibroblasts. (D) Data points are the mean \pm SE of the number of oscillations measured over the first 400 s after histamine application, plotted against the logarithm of histamine concentration. The continuous curve was obtained by fitting the data to Eq. 1, as shown in Materials and methods, which yielded EC_{50} values of 2.38 μM .

$[\text{Ca}^{2+}]_i$ at very low concentrations, such as 100 and 300 nM. The Ca^{2+} response to histamine appeared at 1–3 μM ; at these concentrations, the Ca^{2+} signal arising in most WI-38 cells displayed a single peak in response to agonist stimulation. However, at 10 μM histamine, the Ca^{2+} peak was followed by a short train of consecutive Ca^{2+} oscillations. The number of oscillations over 60 min of histamine application was increased at histamine concentrations ranging from 30 μM up to 1 mM. The non-cumulative concentration-response curve of histamine-induced elevation in $[\text{Ca}^{2+}]_i$ is depicted in Figure 2B (black circles), which shows that the increase in histamine concentration produces an increase in the amplitude of the initial Ca^{2+} response (peak). The maximum increase in the peak amplitude was observed at concentrations higher than 300 μM , whereas raising histamine concentration up to 1 mM did not significantly augment the magnitude of the response. Slight stimulation occurred at 3 μM , while no effect was detectable at concentrations lower than 1 μM (100 nM and 300 nM). The concentration of histamine required to produce a half maximal response (EC_{50}), which was calculated by fitting the concentration-response curve as described in Materials and Methods, was 4.96 μM (Figure 2B, black circles). Likewise, in cells

that presented a plateau in the Ca^{2+} waveform, the EC_{50} of the plateau amplitude was equal to 5.25 μM (Figure 2B, blue circles). In order to assess whether the pattern of the Ca^{2+} signal was dependent on histamine concentration, the frequency of each Ca^{2+} signature detected at each histamine concentration (100 nM–1 mM) was calculated (Figure 2C). The data indicate that the spike pattern (see Figures 1A, 2C) is more common when fibroblasts are stimulated with low histamine concentrations (100 nM–1 μM), whereas the spike-oscillations patterns is more frequent as the histamine concentration is increased (3 μM –1 mM) (see Figures 1B,C, 2B). In accord, the number of oscillations recorded over the first 400 s after histamine application was increased in a histamine concentration-response manner with a EC_{50} = 2.37 μM (Figure 2D).

Desensitization of the Ca^{2+} response by repeated stimulation of WI-38 human lung fibroblasts with histamine

Homologous desensitization is a feature of GqPCRs, including H1R (Chen et al., 2014; Burghi et al., 2021).

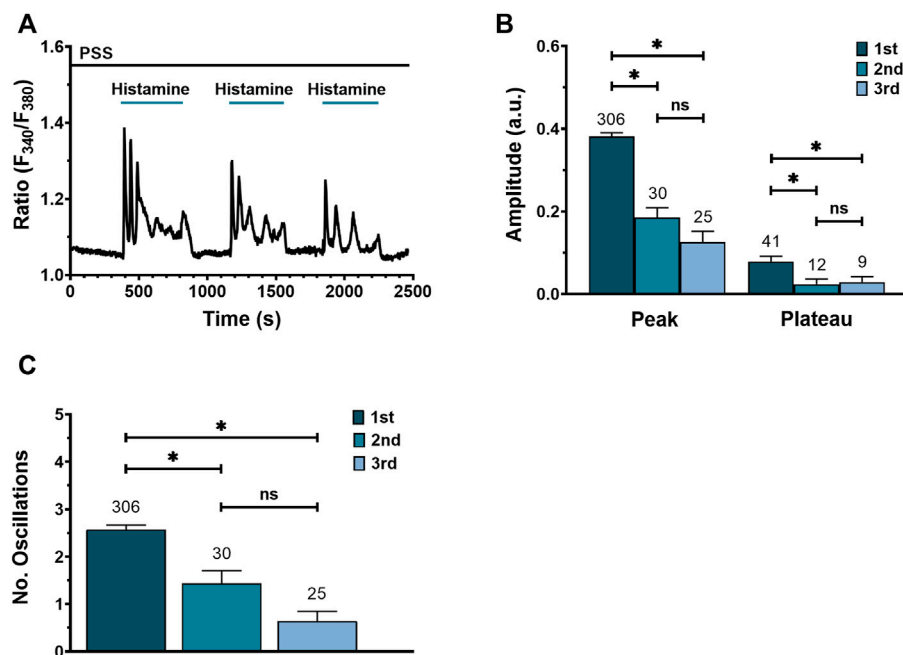


FIGURE 3

Effect of consecutive histamine applications on Ca^{2+} signal in WI-38 human lung fibroblasts WI-38. **(A)** Representative recording of a triple application of histamine ($300 \mu\text{M}$) in one cell, each followed by a washout with physiological saline solution (PSS). **(B)** Mean \pm SE of peak and plateau amplitudes of the Ca^{2+} transient evoked by 3 consecutive histamine applications: first application (1st), second application (2nd), third application (3rd). **(C)** Mean \pm SE of the number of oscillations measured over 400 s after each histamine application. The number in the figure represents the number of cells studied. Comparison between groups was performed using the Kruskal–Wallis test (* = $p \leq 0.05$; ns = no statistically relevant differences between groups).

Figure 3A shows a typical Ca^{2+} recording from a WI-38 fibroblast exposed to three consecutive applications of $300 \mu\text{M}$ histamine followed by PSS washout. Histamine elicited a similar Ca^{2+} response consisting in an initial Ca^{2+} peak followed by sustained plateau, superimposed by Ca^{2+} oscillations. However, the peak and plateau amplitudes (Figure 3B), as well as the number of oscillations (Figure 3C), were significantly reduced by repetitive histamine stimulation. These data suggest that the application of a maximal concentration of histamine ($300 \mu\text{M}$) to the same fibroblast leads to receptor desensitization.

Histamine-evoked elevation in $[\text{Ca}^{2+}]_i$ in WI-38 human lung fibroblasts is primarily mediated through activation of H1R and to a lesser extent through H2R

In order to elucidate the HR subtype through which histamine triggers an intracellular Ca^{2+} signal in WI-38 human lung fibroblasts, specific HR antagonists were used: for H1Rs pyrilamine ($100 \mu\text{M}$), for H2Rs ranitidine ($50 \mu\text{M}$),

for H3R clobenpropit ($50 \mu\text{M}$) and, finally, for the H4R receptor, NJ7777120 ($10 \mu\text{M}$). After 30 min preincubation and in the continuous presence of the histaminergic antagonists, histamine ($300 \mu\text{M}$) was applied as indicated by the green bars. In order to confirm cell viability, arachidonic acid (AA) $50 \mu\text{M}$ was applied in cells in which histamine failed to induce an increase in $[\text{Ca}^{2+}]_i$ (Berra-Romani et al., 2019). Pharmacological manipulation of HR in WI-38 human lung fibroblasts revealed that H1R blockage completely abolished the histamine-evoked Ca^{2+} signal (Figure 4A), H2R blockage significantly decreased the amplitude of the Ca^{2+} signal (Figure 4B), while H3R (Figure 4C) and H4R blockage (Figure 4D) had no significant effect. In Figure 4E, the statistical comparison between the mean \pm SE peak amplitude of the Ca^{2+} signals evoked by histamine $300 \mu\text{M}$ in the absence (Ctrl) and presence of the different antihistaminergic receptors antagonists (H1R, H2R, H3R, and H4R) are summarized. These results indicate that, for the $[\text{Ca}^{2+}]_i$ elevation to take place in the lung fibroblast cell line, WI-38, the activation of mainly H1R and, to a lesser extent, H2R is necessary, whereas H3R and H4R seem to play no role.

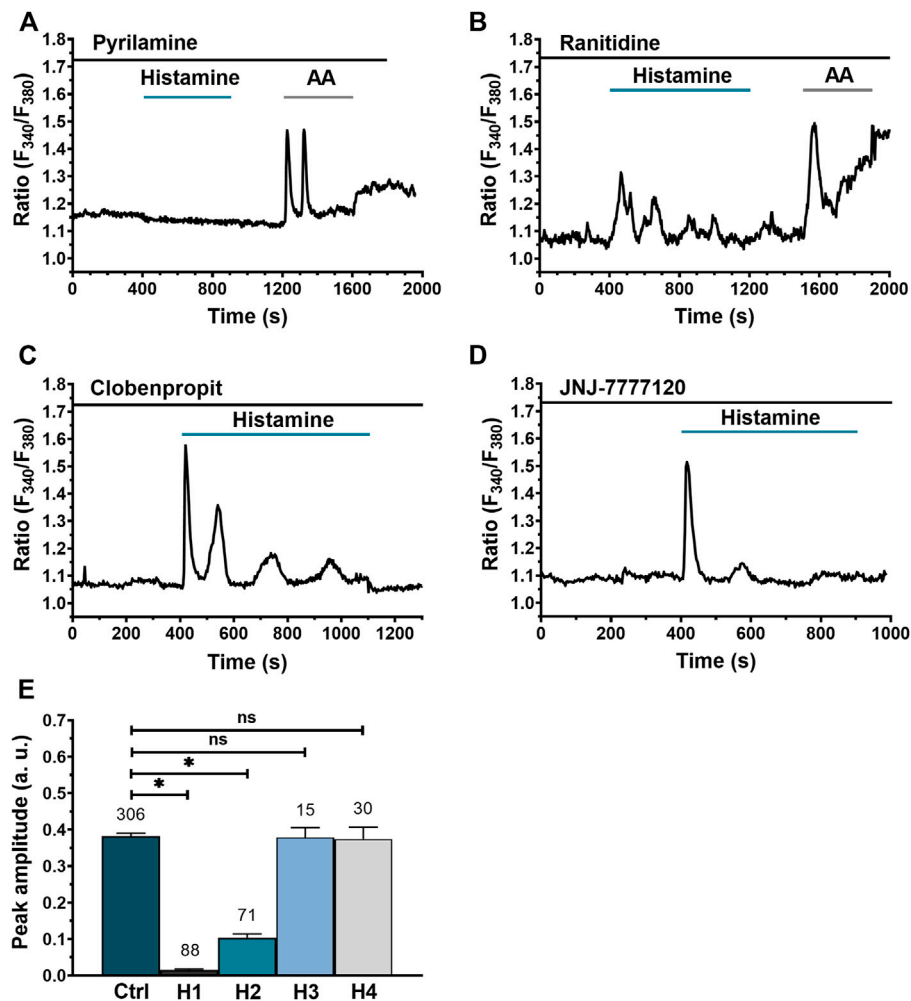


FIGURE 4

Dissection of histaminergic receptors (HR) responsible for histamine-evoked Ca²⁺ signal in WI-38 human lung fibroblasts. (A) Typical recording of histamine-evoked Ca²⁺ signal in the presence of the H1R antagonist, pyrillamine (100 μM). (B) Typical recording of the histamine-evoked Ca²⁺ signal in the presence of the H2R antagonist, ranitidine (50 μM). (C) Typical recording of the histamine-evoked Ca²⁺ signal in the presence of the H3R antagonist, clobenpropit (50 μM). (D) Typical recording of histamine-evoked Ca²⁺ signal in the presence of H4R antagonist, JNJ-777120 (10 μM). All histaminergic antagonists were preincubated for 30 min prior to histamine application (incubation time not shown). For experiments showed in (A,C), arachidonic acid (AA 50 μM) was applied after histamine application to corroborate cell viability. (E) Mean ± SE of the peak amplitude of the Ca²⁺ transient evoked by histamine (300 μM) in the absence (Ctrl) and presence of the HR antagonists: pyrillamine 100 μM (H1), ranitidine 50 μM (H2), clobenpropit 50 μM (H3) and JNJ-777120 10 μM (H4). The numbers in the figure represents the number of cells studied. Comparison between groups was performed using the Kruskal–Wallis test (* = p ≤ 0.05) (ns = no statistically relevant differences between groups).

Histamine-evoked Ca²⁺ signals in WI-38 lung fibroblasts do not involve Gα_{i/o} activation but require PLCβ recruitment and ER Ca²⁺ release

The results shown in Figures 4C–E suggest that H3R and H4R do not participate in histamine-activated Ca²⁺ signaling. H3R and H4R are canonically coupled to Gα_{i/o} proteins (Haas et al., 2008). Therefore, a reliable strategy to corroborate the lack of H3R and H4R involvement in histamine response would be to demonstrate that pertussis toxin (PT), a selective

inhibitor of Gα_{i/o} protein signalling, does not modify histamine-evoked Ca²⁺ signals. Indeed, as shown in Figure 5A, preincubation (30 min) with 100 ng/ml PT did not prevent histamine from increasing intracellular [Ca²⁺]_i in WI-38 fibroblasts. In accord, the amplitude of initial Ca²⁺ transient (peak) was not statistically different from untreated cells (Figure 5B). These results confirm that histamine-evoked increase in [Ca²⁺]_i in human lung WI-38 fibroblasts is insensitive to the inhibition of Gα_{i/o} by PT (Figures 5A,B). After confirming that H1R and H2R are involved in the Ca²⁺ response to histamine, we turned to dissect out the molecular

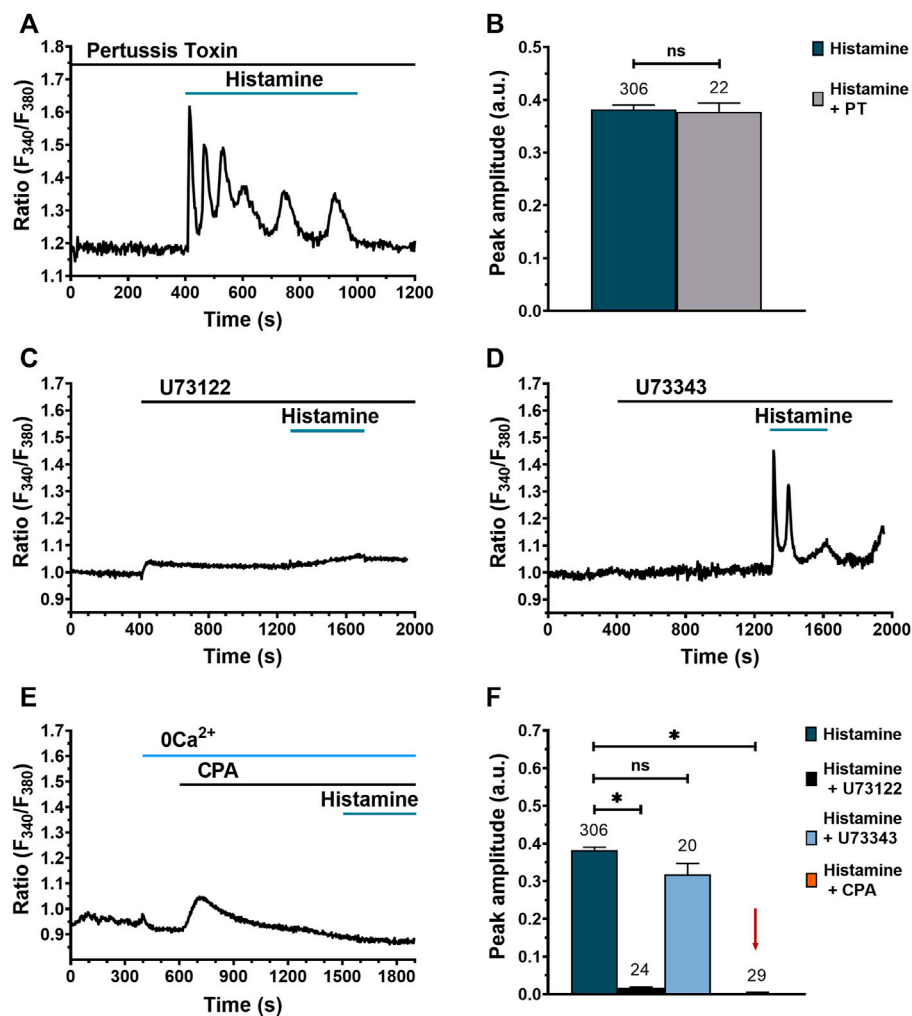


FIGURE 5

Histamine-evoked Ca^{2+} signals in WI-38 human lung fibroblasts do not involve $\text{G}\alpha_{i/o}$ activation but require PLC and ER Ca^{2+} release. (A) Typical recording of the Ca^{2+} response to histamine (300 μM) in fibroblasts preincubated for 30 min with 100 ng/ml pertussis toxin (PT). (B) Mean \pm SE of the peak amplitude of histamine-evoked Ca^{2+} transients in the absence (green bar) and presence of pertussis toxin (gray bar). Comparison between groups was performed using the Student's t-test (ns = no statistically relevant differences between groups). (C) Typical recording of the effect of histamine (300 μM) on Ca^{2+} signal in cells pretreated for 15 min with U73122 (10 μM), a specific PLC inhibitor. (D) Typical recording of the Ca^{2+} response to histamine (300 μM) in cells pretreated for 15 min with U73343 (10 μM), an inactive analog of U73122. (E) Representative recording of the Ca^{2+} signal evoked by histamine (300 μM) in cells pretreated with CPA (10 μM) in the absence of extracellular Ca^{2+} (0Ca^{2+}). (F) Mean \pm SE of the peak Ca^{2+} response to histamine (300 μM ; green bar) in the presence of U73122 10 μM (black bar), U73343 10 μM (blue bar) and CPA 10 μM (orange bar not visible, marked with a red arrow). The numbers in the figure represent the number of cells studied. Statistical comparison between groups was performed using ANOVA test (* = $p \leq 0.05$).

underpinnings of the Ca^{2+} transient by using the following drugs: 1) U73122 (10 μM), a selective inhibitor of PLC (Moccia et al., 2006; Berra-Romani et al., 2012; Berra-Romani et al., 2020); 2) U73343 (10 μM), an inactive analogue of U73122 (Guzmán-Silva et al., 2015); and 3) cyclopiazonic acid (CPA) (10 μM), a selective inhibitor of sarco-edoplasmic reticulum calcium ATPase (SERCA) pump (Guzmán-Silva et al., 2015; Berra-Romani et al., 2020). The

results obtained showed that PLC inhibition upon preincubation (15 min) with U73122 suppresses histamine-evoked Ca^{2+} signal (Figures 5C,F), whereas its inactive analog, U73343, does not affect the Ca^{2+} response (Figures 5D,F). Likewise, ER emptying *via* Ca^{2+} leak channels after SERCA inhibition with CPA in an extracellular Ca^{2+} -free environment (0Ca^{2+}) prevented the Ca^{2+} response to histamine (Figures 5E,F). These results indicate that the Ca^{2+} transient generated

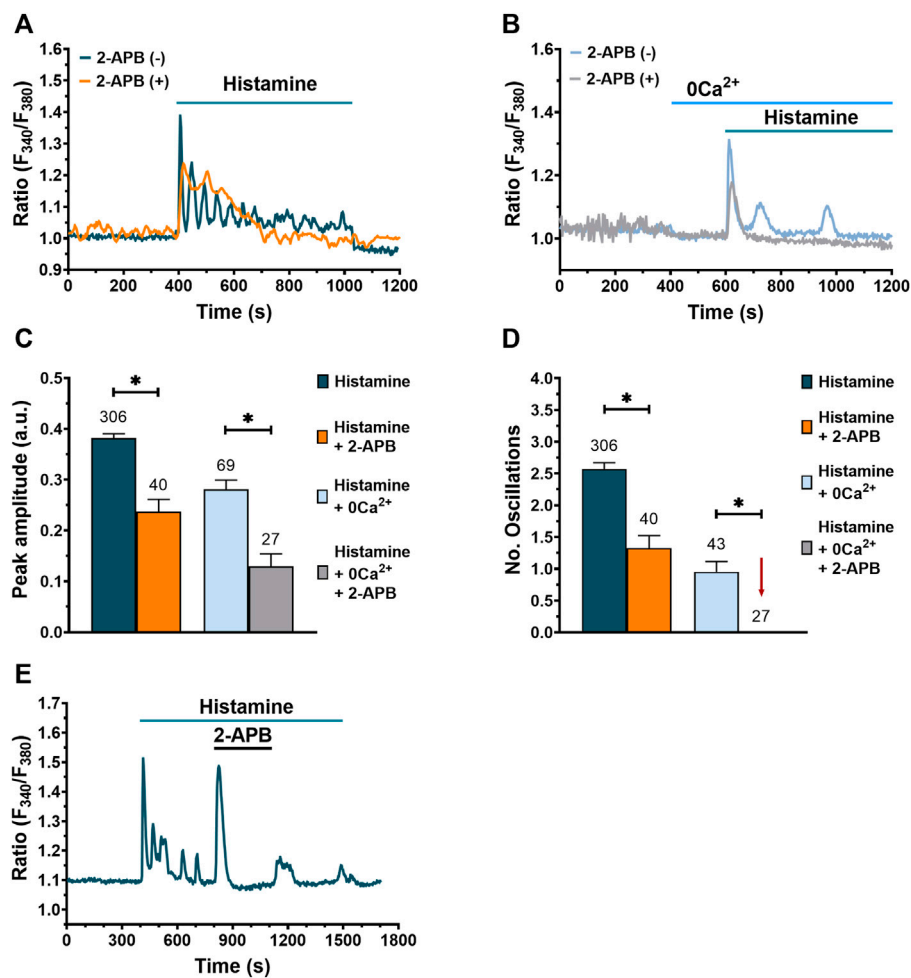


FIGURE 6

Involvement of $InsP_3R$ in histamine-evoked Ca^{2+} signals in WI-38 human lung fibroblasts. (A) Typical recording of the Ca^{2+} response to histamine (300 μM) in fibroblasts pre-incubated with 2-APB (50 μM) for 20 min [orange trace, 2-APB (+)] and its control [dark green trace, 2-APB (-)]. (B) Typical recording of histamine-evoked Ca^{2+} signal in absence of extracellular Ca^{2+} (0 Ca^{2+}) after pre-incubation of fibroblasts for 20 min with 2-APB (50 μM) [gray trace, 2-APB (+)] and its control [blue trace, 2-APB (-)]. In (A, B) basal Ca^{2+} levels were aligned for comparative purposes. (C) Mean \pm SE of the peak amplitude of the Ca^{2+} response to histamine (300 μM) in normal extracellular Ca^{2+} and in absence (dark green bar) or presence of 50 μM 2-APB (orange bar). Mean \pm SE of the peak amplitude of the Ca^{2+} response to histamine (300 μM) in absence of extracellular Ca^{2+} (0 Ca^{2+}) and in absence (blue bar) or presence of 50 μM 2-APB (gray bar). Statistic comparison between groups was performed using Mann-Whitney and t-Student test respectively ($* = p \leq 0.05$). (D) Mean \pm SE of the number of oscillations evoked by histamine (300 μM) in normal extracellular Ca^{2+} and in absence (dark green bar) or presence of 50 μM 2-APB (orange bar). Mean \pm SE of the number of oscillations evoked by histamine (300 μM) in the absence of extracellular Ca^{2+} (0 Ca^{2+}) and in absence (blue bar) or presence of 50 μM 2-APB (gray bar, gray bar not visible, marked with a red arrow). Statistical comparison between groups was performed using Mann-Whitney and t-Student test respectively ($* = p \leq 0.05$). The numbers in the figure represents the number of cells studied. (E) Typical recording of the Ca^{2+} signal evoked by histamine and the effect of 2-APB application.

after histamine stimulation in WI-38 human lung fibroblasts is due to PLC activation and Ca^{2+} release from the ER.

InsP₃R play an important role in histamine-evoked Ca^{2+} signaling in WI-38 human lung fibroblasts

Having demonstrated that the ER Ca^{2+} stores contributes to histamine-evoked Ca^{2+} signals upon PLC activation, we

evaluated the involvement of $InsP_3R$, which provides the main pathway for ER Ca^{2+} release in fibroblasts (Horie et al., 2014; Berra-Romani et al., 2020). The results obtained demonstrate that, after incubation for 20 min with 2-aminoethoxydiphenyl borate (2-APB, 50 μM), a drug widely used as $InsP_3R$ inhibitor (Guzmán-Silva et al., 2015), the amplitude of histamine-evoked initial Ca^{2+} transient is significantly reduced compared to untreated cells, both in the presence (Figures 6A,C) and in the absence of extracellular Ca^{2+} (Figures 6B,C). In addition,

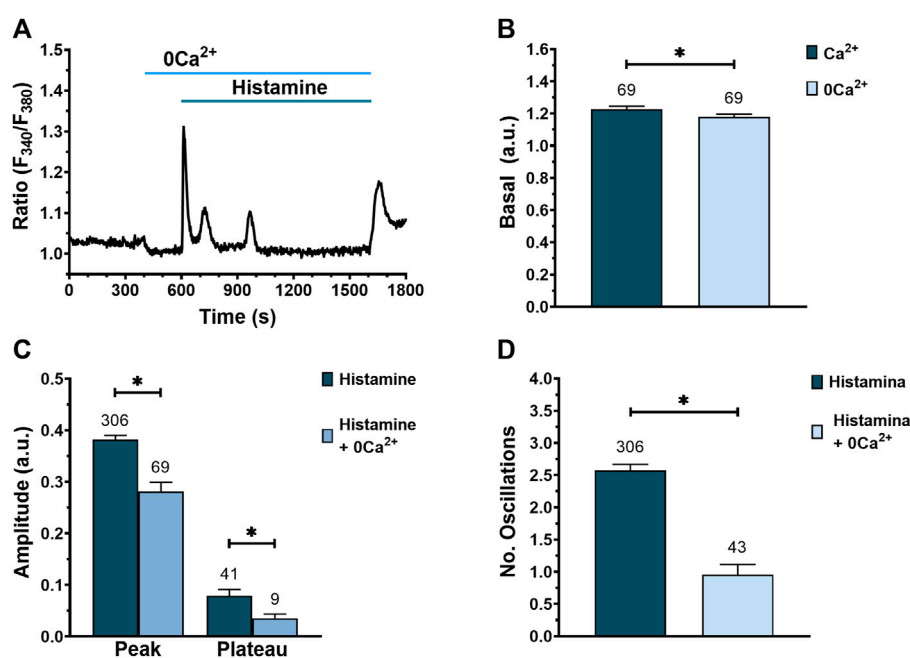


FIGURE 7

Effect of extracellular Ca²⁺ removal on histamine-evoked Ca²⁺ signal in WI-38 human lung fibroblasts. (A) Typical recording of histamine-evoked Ca²⁺ signals in the absence of extracellular Ca²⁺ (0Ca²⁺). (B) Mean ± SE of basal [Ca²⁺]_i in fibroblasts exposed to an extracellular solution with (dark green bar) or without extracellular Ca²⁺ (blue bar). Comparison between groups was performed using the t-Student test (* = *p* ≤ 0.05). (C) Mean ± SE of peak and plateau amplitudes of the Ca²⁺ signal evoked by histamine in fibroblasts exposed to an extracellular solution with (dark green bar) or without extracellular Ca²⁺ (blue bar). Comparison between groups was performed using the t-Student test for peak amplitude data and Mann-Whitney test for plateau amplitude data (* = *p* ≤ 0.05). (D) Mean ± SE of the number of oscillations recorded during the first 400 s after histamine application in an extracellular solution with (dark green bar) or without extracellular Ca²⁺ (blue bar). Comparison between groups was performed using the Mann-Whitney test (* = *p* ≤ 0.05). The numbers in the figures represent the number of cells studied.

the number of oscillations was significantly decreased when fibroblasts were preincubated with 2-APB in normal Ca²⁺ (Figures 6A,D) and completely eliminated under 0Ca²⁺ conditions (Figures 6B,D). Even though 2-APB application during histamine-activated Ca²⁺ oscillations caused an immediate and transitory increase in [Ca²⁺]_i, 2-APB subsequently erased the intracellular Ca²⁺ oscillations and plateau phase; this effect was reversible (Figure 6E). RyR could support InsP₃-induced intracellular Ca²⁺ oscillations through CICR, as reported in other cell types (Paltauf-Doburzynska et al., 2000). Nevertheless, the acute addition of caffeine (10 mM) mimicked the inhibitory effect of 2-APB by reversibly interrupting the oscillatory Ca²⁺ train (Supplementary Figure S1) in 92.3% of tested cells (60 out of 65 cells). This observation confirms that RyR, which are directly gated by caffeine (Pulina et al., 2010), do not contribute to histamine-induced intracellular Ca²⁺ waves in WI-38 fibroblasts and is consistent with the well-known phenomenon of InsP₃R inhibition by caffeine (Parker and Ivorra, 1991; Moccia et al., 2003). Taken together, these results suggest a strong involvement of InsP₃R in

histamine-evoked Ca²⁺ transients in lung fibroblasts of the WI-38 cell line.

Extracellular Ca²⁺ influx contributes to histamine-induced intracellular Ca²⁺ signaling in WI-38 human lung fibroblasts

Next, we evaluated the contribution of extracellular Ca²⁺ to histamine-evoked Ca²⁺ signals by exposing the WI-38 fibroblasts to histamine in the absence of external Ca²⁺ to prevent Ca²⁺ entry across the plasma membrane (Berra-Romani et al., 2020). Histamine elicited an immediate increase in [Ca²⁺]_i in the absence of extracellular Ca²⁺ in 66 of 69 cells (Figure 7A). Of note, exposure of WI-38 cells to 0Ca²⁺ conditions caused a significant reduction in basal [Ca²⁺]_i (Figures 7A,B), which is consistent with the presence of a constitutive Ca²⁺ entry pathway (Zuccolo et al., 2018). When histamine (300 μM) was applied to fibroblasts under 0Ca²⁺ conditions, the peak and plateau amplitudes (Figure 7C), as well as the number of intracellular Ca²⁺

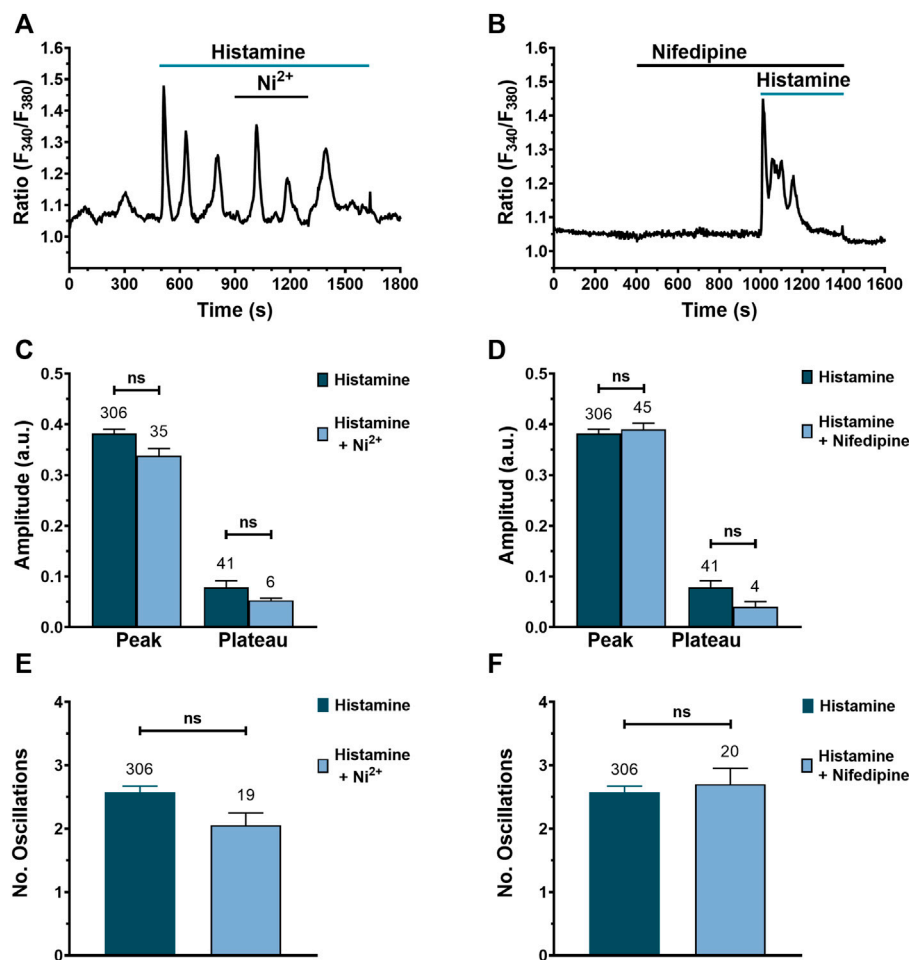


FIGURE 8

Blocking Ca^{2+} entry through VOCs does not affect histamine-evoked intracellular Ca^{2+} signals in WI-38 human lung fibroblasts. (A) Typical recording of histamine-evoked Ca^{2+} signals in the presence of nickel ($10 \mu\text{M}$). (B) Typical recording of histamine-evoked Ca^{2+} signals in the presence of nifedipine ($10 \mu\text{M}$). Comparison between groups was performed using the Mann-Whitney test (ns = not statistics differences between groups). (C) Mean \pm SE of the peak and plateau amplitudes of the Ca^{2+} response to histamine ($300 \mu\text{M}$) in absence (dark green bar) or presence of the non-specific VOC inhibitor, nickel $10 \mu\text{M}$ (blue bar). (D) Mean \pm SE of the peak and plateau amplitudes of the Ca^{2+} response to histamine ($300 \mu\text{M}$) in absence (dark green bar) or presence of the specific VOC inhibitor, nifedipine $10 \mu\text{M}$ (blue bar). (E) Mean \pm SE of the number of oscillations recorded during the first 400 s after histamine application in presence (dark green bar) or presence of the unspecific VOC inhibitor, nickel $10 \mu\text{M}$ (blue bar). (F) Mean \pm SE of the number of oscillations recorded during the first 400 s after histamine application in presence (dark green bar) or absence of the specific VOC inhibitor, nifedipine $10 \mu\text{M}$ (blue bar).

oscillations (Figure 7D), were significantly reduced compared to control conditions. In particular, Ca^{2+} oscillations rapidly run down in the absence of Ca^{2+} entry (Figure 7A). Furthermore, ongoing Ca^{2+} oscillations reversibly ceased upon removal of extracellular Ca^{2+} (Supplementary Figure S2) in 97.1% of tested cells (66 out of 68 cells). These results indicate that the peak and plateau amplitude as well the number of Ca^{2+} oscillations evoked by histamine are due to both Ca^{2+} release from the ER and Ca^{2+} influx from the extracellular medium.

Blocking Ca^{2+} entry through VOCs does not affect histamine-evoked intracellular Ca^{2+} signals

There is evidence for a key role of L-type VOCs in TGF- β -induced Ca^{2+} signaling in human lung fibroblasts (Mukherjee et al., 2015). We, therefore, evaluated their involvement in histamine-induced intracellular Ca^{2+} signaling in WI-38 cells. We exploited a non-specific L-type VOC antagonist (nickel, $10 \mu\text{M}$) (Figures 8A,C,E) and a specific VOC antagonist

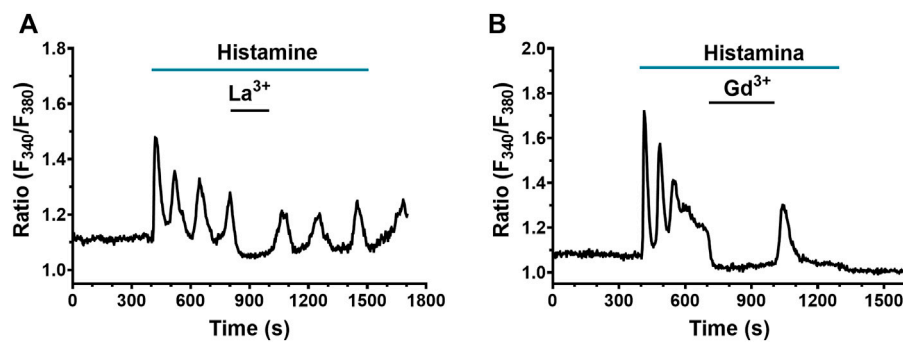


FIGURE 9

Effect of SOCE blockade on histamine-evoked Ca^{2+} signals in WI-38 human lung fibroblasts. (A) Typical recording of histamine-evoked Ca^{2+} signals and effect of the application of $10 \mu\text{M}$ La^{3+} ($n = 79$). (B) Typical recording of histamine-evoked Ca^{2+} signals and effect of the application of $10 \mu\text{M}$ Gd^{3+} ($n = 40$).

(nifedipine, $10 \mu\text{M}$) (Figures 8B,D,F). The results show that there were no significant differences in the peak and plateau amplitudes, as well as in the number of oscillations, when Ca^{2+} entry through VOCs was inhibited with either nickel (Hobai et al., 2000) or nifedipine (Zhang et al., 2007), respectively.

Ca^{2+} influx through SOCs plays an important role in the plateau and oscillations of histamine-evoked Ca^{2+} transients in WI-38 lung fibroblasts

A recent investigation hinted at SOCE as the main Ca^{2+} entry pathway sustaining the Ca^{2+} response to chemical stimuli in human lung fibroblasts (Guzmán-Silva et al., 2015). Therefore, we evaluated the role of SOCs in the Ca^{2+} signal evoked by histamine in WI-38 fibroblasts. The pyrazole-derivative, BTP-2, which is widely employed to inhibit SOCE in non-excitable cells (Prakriya and Lewis, 2015; Moccia et al., 2016; Zhang et al., 2020), increases $[\text{Ca}^{2+}]_i$ in human lung fibroblasts (Guzmán-Silva et al., 2015) and cannot be reliably used to assess SOCE involvement in histamine-evoked extracellular Ca^{2+} entry. In accord, Supplementary Figure S3 shows that BTP-2 ($20 \mu\text{M}$) induced an immediate elevation in $[\text{Ca}^{2+}]_i$ upon application during the decay phase of the initial Ca^{2+} response to histamine. However, low micromolar doses of the trivalent cations, La^{3+} and Gd^{3+} , can also selectively inhibit Orai channels, which provides the main pore-forming subunits of SOCs in both excitable and non-excitable cells (Prakriya and Lewis, 2015; Moccia et al., 2016; Zhang et al., 2020), including human lung fibroblasts (Guzmán-Silva et al., 2015; Vazquez-de-Lara et al., 2018). The results showed that the application of both La^{3+} ($10 \mu\text{M}$) and Gd^{3+} ($10 \mu\text{M}$) abrogated the plateau and

Ca^{2+} oscillations in 79 and 40 cells exposed to La^{3+} and Gd^{3+} , respectively (Figure 9A,B). This effect was reversible upon removal of La^{3+} or Gd^{3+} . Intriguingly, the acute addition of La^{3+} and Gd^{3+} also caused a decrease in resting Fura-2 fluorescence ratio below the baseline, which suggests that Orai channels are involved in constitutive Ca^{2+} entry (see Figure 6B). In summary, these results suggest a strong involvement of Ca^{2+} entry through SOCs in the histamine-evoked Ca^{2+} transient in lung fibroblasts of the WI-38 cell line.

Preliminary characterization of the Ca^{2+} handling machinery in in WI-38 fibroblast

No comprehensive information is available regarding the molecular composition of the Ca^{2+} handling toolkit in WI-38 fibroblasts. Therefore, we performed a preliminary qRT-PCR analysis of the main Ca^{2+} -permeable channels that are known to shape the Ca^{2+} response to histamine in other cell types. We used the specific primers described in Table 1, while negative controls were carried out by excluding the reverse transcription reaction, as shown in (Negri et al., 2021). Figure 10 displays that WI-38 lung fibroblasts express the transcripts encoding for all the InsP_3R isoforms, i.e., $\text{InsP}_3\text{R}1$, $\text{InsP}_3\text{R}2$, and $\text{InsP}_3\text{R}3$, whereas, among the molecular players of the SOCE machinery, only $\text{STIM}2$ and $\text{Orai}3$ paralogues were present. In addition, the mRNAs encoding for $\text{RyR}1$ and most of the members of the Transient Receptor Potential Canonical (TRPC) subfamily, i.e., $\text{TRPC}1$, $\text{TRPC}3$, $\text{TRPC}4$, $\text{TRPC}5$, and $\text{TRPC}6$ (Negri et al., 2019), were also found (Figure 10). Therefore, these findings support the notion that the interaction between InsP_3R and SOC drive histamine-induced intracellular Ca^{2+} signals in WI-38 human adult lung fibroblasts.

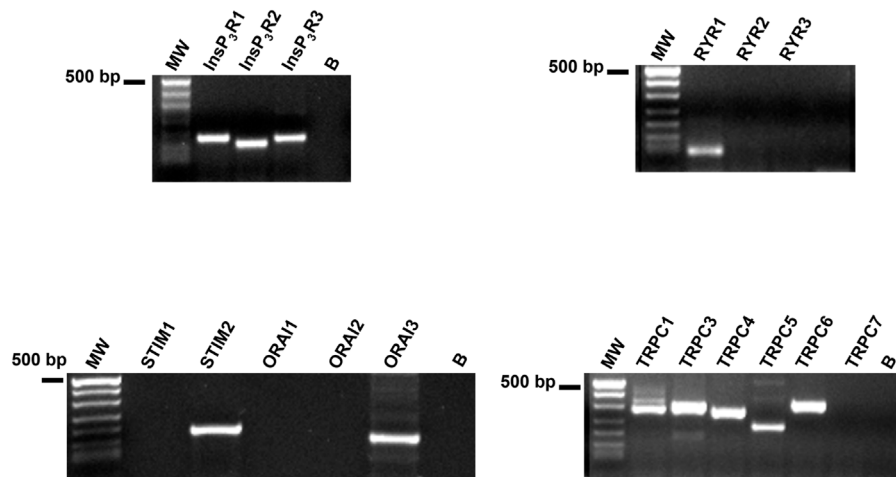


FIGURE 10

Transcriptomic characterization of the Ca^{2+} handling machinery in WI-38 fibroblasts. Gel electrophoresis of the PCR products are shown. Electrophoresis was performed as indicated in Materials and Methods. The PCR products were of the expected size: InsP_3R_1 , 180 bp; InsP_3R_2 , 158 bp; InsP_3R_3 , 173 bp; RyR_1 , 75 bp; TRPC_1 , 307 bp; TRPC_3 , 336 bp; TRPC_4 , 300 bp; TRPC_5 , 221 bp; TRPC_6 , 341 bp; STIM_2 , 186 bp; and Orai_3 , 159 bp. No signal was observed for STIM_1 and Orai_1 . MW, molecular weight markers. B, reaction without the template.

Discussion

Pulmonary remodeling is the main long-term complication of asthma and occurs as a compensatory response to a persistent inflammatory state of the lower airway epithelium that leads to an irreversible restriction in the airflow, and is a result of a multi-step process known as “scarring.” Mast cells play a crucial pathogenic role in asthma by releasing the autacoid mediator histamine, which stimulates airway smooth muscle cell constriction and hyperplasia, and activates fibroblasts to acquire a contractile phenotype and support pulmonary remodeling. The molecular mechanisms whereby histamine promotes fibroblast proliferation and migration is still unclear, although preliminary evidence indicates that histamine-induced collagen gel contraction is mediated by an increase in $[\text{Ca}^{2+}]_i$ (Horie et al., 2014). Intriguingly, it has long been known that intracellular Ca^{2+} signaling can adopt multiple patterns to orchestrate many of the cellular events that contribute to pulmonary remodeling, including fibroblast proliferation and transformation into myofibroblasts (Janssen et al., 2015). Herein, we provided the first clear-cut characterization of the signaling pathways that shape histamine-induced intracellular Ca^{2+} signals in the WI-38 cell line, which is widely employed to study human lung fibroblasts. Our findings could pave the way towards an alternative strategy to target histamine signaling and thereby dampen airway remodeling in asthma.

Intracellular Ca^{2+} signals regulate a broad spectrum of cellular processes by adopting diverse spatiotemporal dynamics, ranging from single Ca^{2+} transient to repetitive Ca^{2+} transients whose frequency depends on agonist strength

(Smedler and Uhlén, 2014). The introduction of high-speed microfluorimetry and high-resolution image analysis techniques have allowed researchers to monitor changes in $[\text{Ca}^{2+}]_i$ in individual cells simultaneously. These techniques have revealed a surprising degree of heterogeneity in the Ca^{2+} responses to the same agonist generated even by cells in the same field of view. Herein, we report that histamine evoked complex Ca^{2+} waveforms in WI-38 fibroblasts that could be classified according to the following patterns: 1) peak, 2) peak and oscillations, 3) peak plateau and oscillations, and 4) peak and plateau. Spatial and temporal heterogeneity of the Ca^{2+} signature can be a hallmark of the Ca^{2+} response evoked by both mechanical (Berra-Romani et al., 2008; Jing et al., 2013) and chemical cues (Dupont and Combettes, 2016; Wacquier et al., 2019). A recent investigation showed that, in normal human lung fibroblasts (NHLF), beractant (a natural surfactant) induced distinct patterns of intracellular Ca^{2+} signals, each comprising an initial Ca^{2+} spike that could be followed either by a) transient, by repetitive Ca^{2+} oscillations, c) a sustained Ca^{2+} plateau or d) a sustained plateau overlapped by repetitive Ca^{2+} oscillations (Guzmán-Silva et al., 2015). Similarly, ATP could elicit either a single Ca^{2+} transient or recurring Ca^{2+} oscillations in NHLF (Janssen et al., 2015), whereas a heterogeneous array of agonist-induced intracellular Ca^{2+} signals has been described in fibroblasts deriving from other tissues (Chen et al., 2010; Kemény et al., 2013; Lembong et al., 2015). As expected (Ong et al., 2019), the diverse Ca^{2+} dynamics and the number of oscillations depend on histamine concentration, with the lower concentration being dominated by the peak pattern and the higher concentration being dominated by the peak, plateau

and oscillations pattern. In accord, low doses of histamine are predicted to elicit only intracellular Ca^{2+} release, while the Ca^{2+} response to higher doses can also involve extracellular Ca^{2+} entry (Ong et al., 2019). Likewise, a recent investigation showed that histamine was more eager to induce 1 or 2 Ca^{2+} spikes at low picomolar doses, whereas the number and frequency of repetitive Ca^{2+} transients progressively increased with histamine concentration (up to 300 μM) in human microvascular endothelial cells (Berra-Romani et al., 2020). The non-cumulative concentration-response relationship showed that the Ca^{2+} signal evoked by histamine in WI-38 human lung fibroblasts present an EC_{50} value of 4.96 μM , a maximum concentration of 300 μM , and a threshold concentration of 100 nM. Similarly, histamine induced collagen gel contraction and proliferation in, respectively, primary cultured human lung fibroblasts (Horie et al., 2014) and IMR-90 adult lung fibroblasts (Kunzmann et al., 2007) within a concentration range spanning from 100 nM up to 100 μM . Moreover, the pro-migratory effect of histamine on human lung fetal fibroblasts appeared at a threshold dose of 100 nM (Kohyama et al., 2010). These studies concur with the evidence that H1R mediates histamine-induced proliferation, migration, and collagen gel contraction in human lung fibroblasts. In agreement with these observations, pharmacological manipulation showed that histamine generates a complex increase in $[\text{Ca}^{2+}]_i$ in WI-38 fibroblasts mainly through H1R and, to a lesser extent, through H2R. Furthermore, short-term exposure of the cells to histamine reduced the responsiveness to subsequent applications of the agonist, which is a hallmark of H1R signalling (Smit et al., 1992). Homologous desensitization of H1R has also been reported in smooth muscle preparations (Leurs et al., 1990; Leurs et al., 1991), HeLa cells (Smit et al., 1992), and human gingival fibroblasts (Gutiérrez-Venegas and Rodríguez-Pérez, 2012). Conversely, H3R and H4R do not seem to play a crucial role in the onset of the Ca^{2+} signal. These results were supported by the evidence that histamine-evoked intracellular Ca^{2+} waves were not altered by the PT-dependent ribosylation of the $\text{G}\alpha_{i/o}$ subunit, which triggers the signalling cascades activated downstream of both H3R and H4R (Seifert et al., 2013). Consistent with our observations, Horie et al. (2014) previously reported the involvement of H1R in histamine-induced collagen gel contraction in primary cultured lung fibroblasts, whereas H2R could be responsible for a small Ca^{2+} response occurring in the presence of diphenhydramine, a specific H1R-antihistamine.

The mechanisms that control the mobilization of cytosolic Ca^{2+} are key to the regulation of numerous eukaryotic cell functions (Clapham, 2007). Therefore, after identifying the HR subtype responsible for histamine-evoked Ca^{2+} signaling, we set out to dissect the molecular underpinnings of the Ca^{2+} transient. H1R is a GqPCR that can signal an increase in $[\text{Ca}^{2+}]_i$ by stimulating PLC β to synthesize InsP_3 and trigger ER Ca^{2+} release through InsP_3R (Berra-Romani et al., 2012; Seifert et al.,

2013; Berra-Romani et al., 2020). In accord, the Ca^{2+} response to histamine still occurred in the absence of extracellular Ca^{2+} , although it rapidly run down after 1-3 Ca^{2+} spikes. Furthermore, histamine-evoked intracellular Ca^{2+} signals were strongly reduced by blocking PLC β activity with U73122, but not its inactive analog, U73343. Furthermore, the initial Ca^{2+} peak was significantly reduced as compared to control, i.e., untreated, cells upon inhibition of InsP_3R with 2-APB. This inhibitory effect was observed both in the presence and in the absence of extracellular Ca^{2+} . 2-APB significantly decreased the number of oscillations under normal Ca^{2+} conditions, while it completely erased the spiking response under 0Ca^{2+} conditions. Of note, inhibition of InsP_3Rs with 2-APB, despite decreasing the amplitude of the Ca^{2+} transients, did not completely eliminate histamine-induced Ca^{2+} signals, as previously reported both in fibroblasts (Horie et al., 2014) and in other cell types (Berra-Romani et al., 2020). Unlike histamine, the Ca^{2+} response to beractant in WI-38 fibroblasts was fully abrogated by 2-APB (Guzmán-Silva et al., 2015). This discrepancy can be explained by invoking several hypotheses. First, the ability of 2-APB to penetrate the cell membrane may significantly vary among different cell types: this feature could explain the high sensitivity to 2-APB observed in some cells, but not in others (Soulsby and Wojcikiewicz, 2002). Second, the degree of 2-APB-dependent inhibition could depend on the histamine concentration employed to characterize the Ca^{2+} response in WI-38 lung fibroblasts. For instance, early work carried out in HeLa cells showed that 100 μM 2-APB was able to completely inhibit the ATP-evoked Ca^{2+} response at all the tested concentrations, while histamine-evoked Ca^{2+} signals were only slightly reduced at high agonist doses (i.e., 100 μM) (Peppiatt et al., 2003). It is likely that a higher concentration of 2-APB is required to block InsP_3R recruited by histamine in WI-38 lung fibroblasts. However, we did not increase 2-APB concentration to avoid the concentration-dependent side-effects that have been associated to this powerful InsP_3R inhibitor, such as SOCE inhibition and SERCA modulation (Gambardella et al., 2021). The primary role of InsP_3R in the Ca^{2+} response to histamine was further corroborated by caffeine, which reversibly inhibited, rather than enhancing, histamine-induced intracellular Ca^{2+} oscillations. At the concentration employed in the present investigation, caffeine can either stimulate RyR (Pulina et al., 2010) or inhibit InsP_3R (Parker and Ivorra, 1991; Moccia et al., 2003). Therefore, the blocking effect of caffeine further confirms that InsP_3R are the main responsible for the rhythmical ER Ca^{2+} release induced by caffeine in WI-38 fibroblasts.

While the complex increase in $[\text{Ca}^{2+}]_i$ is triggered by ER Ca^{2+} mobilization through InsP_3R , the Ca^{2+} response is maintained over time by extracellular Ca^{2+} entry. In accord, removal of external Ca^{2+} resulted in the decrease of the Ca^{2+} peak and Ca^{2+} plateau amplitudes, and in the number of Ca^{2+} oscillations evoked by histamine. These findings concur with previous studies showing that Ca^{2+} influx through the plasma membrane sustains intracellular Ca^{2+}

oscillations induced by HIR stimulation in several cell types, including cerebrovascular endothelial cells (Berra-Romani et al., 2020), HeLa cells (Sauvé et al., 1991), and vascular smooth muscle cells (Espinosa-Tanguma et al., 2011). SOCE is activated upon depletion of the ER Ca^{2+} pool and represents the Ca^{2+} entry pathway that sustains the Ca^{2+} signal induced by agonists stimulation in fibroblasts from different tissues, including human mammary gland (Sadras et al., 2021b), human heart (Chung et al., 2021), human skin (Wu et al., 2019), and human lungs (Guzmán-Silva et al., 2015). It has been nicely documented that low (1–10) micromolar doses of the trivalent cations, La^{3+} and Gd^{3+} , plug the access to the Orai channel inner pore, thereby specifically inhibiting SOCE (Prakriya and Lewis, 2015; Moccia et al., 2016; Zhang et al., 2020). In accord, the application of either SOC blocker at 400 s after histamine application completely abolished the oscillations and suppressed the Ca^{2+} plateau in WI-38 lung fibroblasts. Similar results were achieved by the acute addition of 10 μM La^{3+} and 10 μM Gd^{3+} on the long-lasting elevation in $[\text{Ca}^{2+}]_i$ evoked in the same cells by beractant (Guzmán-Silva et al., 2015). VOC represent an alternative pathway for extracellular Ca^{2+} entry in NHLF, as shown for the intracellular Ca^{2+} oscillations induced by transforming growth factor β (Mukherjee et al., 2015). However, two structurally unrelated VOC inhibitors, i.e., nickel and nifedipine, did not affect histamine-evoked intracellular Ca^{2+} signals in WI-38 cells. We hypothesize that histamine-dependent SOC activation does not depolarize the membrane potential to such an extent to induce VOC activation.

A preliminary qRT-PCR analysis of the Ca^{2+} handling machinery confirmed that WI-38 fibroblasts express all the three known InsP_3R isoform and two of the molecular components required to activate SOCE, i.e., STIM2 and Orai3. These data are therefore consistent with the results provided by the pharmacological manipulation of the Ca^{2+} response. Conversely, all Orai and STIM isoforms were detected in human cardiac fibroblasts (Cendula et al., 2021), in which they support spontaneous Ca^{2+} oscillations (Chen et al., 2010). Intriguingly, Orai3 can be directly activated by 50 μM 2-APB independent from ER Ca^{2+} store depletion (Zhang et al., 2020), which might explain the immediate rise in $[\text{Ca}^{2+}]_i$ that occurs upon 2-APB application in the presence (see Figure 6F) but not in the absence (not shown) of extracellular Ca^{2+} . RyR1 transcript was also found, but it is unlikely to contribute to histamine-evoked intracellular Ca^{2+} signals, as shown by the inhibitory effect of caffeine. WI-38 fibroblasts also express the transcripts encoding for TRPC1-TRPC6, but the pharmacological sensitivity of histamine-evoked Ca^{2+} entry to 10 μM La^{3+} and Gd^{3+} argues against the involvement of TRPC isoforms. Moreover, a recent investigation demonstrated that TRPC channels do not support SOCE in primary murine lung fibroblasts (Bendiks et al., 2020). Conversely, TRPC channels, which present a single-channel conductance that is 1000-fold larger than Orai3, could be activated by transforming growth factor β and thereby lead to VOC activation via strong membrane depolarization (Mukherjee et al., 2015). Quite surprisingly, this was the first molecular

characterization of the Ca^{2+} toolkit in human pulmonary fibroblasts. The selective expression of STIM2 as ER Ca^{2+} sensor might explain the rapid fall in resting $[\text{Ca}^{2+}]_i$ observed upon removal of external Ca^{2+} . In accord, STIM2 is activated only by a mild depletion of the ER Ca^{2+} store and can drive the activation of a constitutive Ca^{2+} influx (Brandman et al., 2007). In agreement with this hypothesis, preliminary evidence showed that μM La^{3+} and Gd^{3+} reduced the basal Ca^{2+} entry, thereby suggesting that SOC also support the resting Ca^{2+} permeability of WI-38 fibroblasts (Sanchez-Collado et al., 2020). It is worth of pointing out that the most frequent Ca^{2+} patterns evoked by high doses of histamine, i.e., mode 2) peak-oscillations, 64.7%, and mode 3) peak-plateau-oscillations, 13.39%, entail the occurrence of intracellular Ca^{2+} oscillations. In agreement with this observation, STIM2 and Orai3 can enhance the percentage of cells showing intracellular Ca^{2+} oscillations upon GqPCR stimulation (Yoast et al., 2020; Emrich et al., 2021). Furthermore, mathematical modelling has shown that, because of their distinct sensitivity to cytosolic Ca^{2+} , $\text{InsP}_3\text{R3}$ may provide a constant release of Ca^{2+} that stimulates $\text{InsP}_3\text{R1}$ and $\text{InsP}_3\text{R2}$ to rhythmically release ER stored Ca^{2+} , whereas SOCE maintains the Ca^{2+} response by ensuring ER Ca^{2+} refilling (Dupont and Croisier, 2010; Dupont, 2014). However, the periodic Ca^{2+} transients transition into a sustained plateau either when $\text{InsP}_3\text{R3}$ expression increases (Okumura et al., 2022) or when ER Ca^{2+} release through $\text{InsP}_3\text{R3}$ is enhanced by the tight coupling with the ER-embedded protein, Jaw1 (Okumura et al., 2022). Therefore, the molecular assortment of the distinct STIM/Orai and InsP_3R isoform, as well as cell-to-cell variability in their expression, subcellular distribution, or posttranslational regulation, could contribute to pattern a heterogeneous array of Ca^{2+} signatures in WI-38 adult lung fibroblast (Ishida et al., 2014; Guzmán-Silva et al., 2015; Bartok et al., 2019; Wilson et al., 2020). Conversely, cell cycle asynchrony is an unlikely explanation of the cell-to-cell heterogeneity of histamine-evoked Ca^{2+} waves because our experiments were performed in fibroblasts devoid of serum for 48 h, which causes cell cycle arrest in G0 phase (Santella, 1998). Similarly, previous studies in fibroblasts and other cell types have reported that this variability in the intracellular Ca^{2+} dynamics is not due to cell cycle asynchrony (Ambler et al., 1988; Byron and Villereal, 1989; Dragoni et al., 2011; Guzmán-Silva et al., 2015; Okumura et al., 2022).

In conclusion, the present investigation showed that histamine induces a dose-dependent increase in $[\text{Ca}^{2+}]_i$ in the widely employed human pulmonary fibroblast cell line, WI-38. The Ca^{2+} signal is mainly triggered by HIR and can adopt multiple signatures, the most common of which encompasses intracellular Ca^{2+} oscillations, which have long been known to stimulate gene expression, proliferation, contraction and migration in human pulmonary fibroblasts (Janssen et al., 2015). The Ca^{2+} response to histamine is triggered by ER Ca^{2+} release through InsP_3R and maintained over time by SOCE activation. These data suggest that the Ca^{2+} handling machinery could provide an alternative molecular target to prevent the pernicious effects of histamine on lung fibroblasts in asthmatic patients, as recently suggested also

for pulmonary hypertension (Bikou et al., 2022), *Streptococcus pneumoniae*-induced lung injury (Ali et al., 2022), and asthma itself (Johnson et al., 2022). Much research remains therefore to be done to assess this issue, although the work presented here provides valuable information for understanding the mechanisms that regulate histamine-evoked Ca^{2+} signaling in lung fibroblasts. A limitation of the present study is that we did not use lung fibroblasts from an asthmatic model or from patients with asthma. Future work will have to compare the effect generated by histamine in lung fibroblasts from normal airways and in lung fibroblasts from asthmatic airways.

Data availability statement

The raw data supporting the conclusion of this article will be made available by the authors, without undue reservation.

Author contributions

RB-R and FM conceived and directed the project in collaboration with MG-C, AL-M, UL, and JA-C. AV-G, JS-G, NC-S, MS, GP, and EH-A performed the experiments and analyzed the data. All authors contributed to the article and approved the submitted version.

Acknowledgments

The authors thank CONCYTEP (Consejo de Ciencia y Tecnología del Estado de Puebla) for financing publication expenses.

References

- Abdulrazzaq, Y. M., Bastaki, S. M. A., and Adeghate, E. (2022). Histamine H_3 receptor antagonists - roles in neurological and endocrine diseases and diabetes mellitus. *Biomed. Pharmacother.* 150, 112947. doi:10.1016/j.biopha.2022.112947
- Ali, M., Zhang, X., LaCanna, R., Tomar, D., Elrod, J. W., and Tian, Y. (2022). MICU1-dependent mitochondrial calcium uptake regulates lung alveolar type 2 cell plasticity and lung regeneration. *JCI Insight* 7 (4), e154447. doi:10.1172/jci.insight.154447
- Ambler, S. K., Poenie, M., Tsien, R. Y., and Taylor, P. (1988). Agonist-stimulated oscillations and cycling of intracellular free calcium in individual cultured muscle cells. *J. Biol. Chem.* 263 (4), 1952–1959. doi:10.1016/S0021-9258(19)77971-X
- Bartok, A., Weaver, D., Golenár, T., Nichtova, Z., Katona, M., Bánsághi, S., et al. (2019). IP_3 receptor isoforms differently regulate ER-mitochondrial contacts and local calcium transfer. *Nat. Commun.* 10 (1), 3726. doi:10.1038/s41467-019-11646-3
- Bendiks, L., Geiger, F., Gudermann, T., Feske, S., and Dietrich, A. (2020). Store-operated Ca^{2+} entry in primary murine lung fibroblasts is independent of classical transient receptor potential (TRPC) channels and contributes to cell migration. *Sci. Rep.* 10 (1), 6812. doi:10.1038/s41598-020-63677-2
- Berra-Romani, R., Faris, P., Negri, S., Botta, L., Genova, T., and Moccia, F. (2019). Arachidonic acid evokes an increase in intracellular Ca^{2+} concentration and nitric

Conflict of interest

The authors declare that the research was conducted in the absence of any commercial or financial relationships that could be construed as a potential conflict of interest.

Publisher's note

All claims expressed in this article are solely those of the authors and do not necessarily represent those of their affiliated organizations, or those of the publisher, the editors and the reviewers. Any product that may be evaluated in this article, or claim that may be made by its manufacturer, is not guaranteed or endorsed by the publisher.

Supplementary material

The Supplementary Material for this article can be found online at: <https://www.frontiersin.org/articles/10.3389/fcell.2022.991659/full#supplementary-material>

SUPPLEMENTARY FIGURE S1

Effect of caffeine on histamine-evoked Ca^{2+} signals in WI-38 human lung fibroblasts. Typical recording of histamine-evoked Ca^{2+} signals and effect of the application of 10 mM caffeine.

SUPPLEMENTARY FIGURE S2

Effect of extracellular Ca^{2+} removal on histamine-evoked Ca^{2+} oscillations in WI-38 human lung fibroblasts. Typical recording of histamine-evoked Ca^{2+} oscillations and effect of extracellular Ca^{2+} removal.

SUPPLEMENTARY FIGURE S3

Effect of BTP-2 on histamine-evoked Ca^{2+} signals in WI-38 human lung fibroblasts. Typical recording of histamine-evoked Ca^{2+} signals and effect of BTP-2 ($n = 76$).

oxide production in endothelial cells from human brain microcirculation. *Cells* 8 (7), E689. doi:10.3390/cells8070689

Berra-Romani, R., Faris, P., Pellavio, G., Orgiu, M., Negri, S., Forcaia, G., et al. (2020). Histamine induces intracellular Ca^{2+} oscillations and nitric oxide release in endothelial cells from brain microvascular circulation. *J. Cell. Physiol.* 235 (2), 1515–1530. doi:10.1002/jcp.29071

Berra-Romani, R., Raqeeb, A., Avelino-Cruz, J. E., Moccia, F., Oldani, A., Speroni, F., et al. (2008). Ca^{2+} signaling in injured *in situ* endothelium of rat aorta. *Cell Calcium* 44 (3), 298–309. doi:10.1016/j.ceca.2007.12.007

Berra-Romani, R., Raqeeb, A., Torres-Jácome, J., Guzman-Silva, A., Guerra, G., Tanzi, F., et al. (2012). The mechanism of injury-induced intracellular calcium concentration oscillations in the endothelium of excised rat aorta. *J. Vasc. Res.* 49 (1), 65–76. doi:10.1159/000329618

Bikou, O., Tharakan, S., Yamada, K. P., Kariya, T., Aguero, J., Gordon, A., et al. (2022). Endobronchial aerosolized AAV1.SERCA2a gene therapy in a pulmonary hypertension pig model: Addressing the lung delivery bottleneck. *Hum. Gene Ther.* 33 (9–10), 550–559. doi:10.1089/hum.2021.274

Brandman, O., Liou, J., Park, W. S., and Meyer, T. (2007). STIM2 is a feedback regulator that stabilizes basal cytosolic and endoplasmic reticulum Ca^{2+} levels. *Cell* 131 (7), 1327–1339. doi:10.1016/j.cell.2007.11.039

- Burghi, V., Echeverría, E. B., Zappia, C. D., Díaz Nebreda, A., Ripoll, S., Gómez, N., et al. (2021). Biased agonism at histamine H₁ receptor: Desensitization, internalization and MAPK activation triggered by antihistamines. *Eur. J. Pharmacol.* 896, 173913. doi:10.1016/j.ejphar.2021.173913
- Byron, K. L., and Villereal, M. L. (1989). Mitogen-induced [Ca²⁺]_i changes in individual human fibroblasts. Image analysis reveals asynchronous responses which are characteristic for different mitogens. *J. Biol. Chem.* 264 (30), 18234–18239. doi:10.1016/s0021-9258(19)84702-6
- Carroll, N. G., Mutavdzic, S., and James, A. L. (2002). Distribution and degranulation of airway mast cells in normal and asthmatic subjects. *Eur. Respir. J.* 19 (5), 879–885. doi:10.1183/09031936.02.00275802
- Cendula, R., Chomaničová, N., Adamičková, A., Gažová, A., Kyselovič, J., and Mátuš, M. (2021). Altered expression of ORAI and STIM isoforms in activated human cardiac fibroblasts. *Physiol. Res.* 70 (1), S21–S30. doi:10.33549/physiolres.934771
- Chen, T. R., Tao, R., Sun, H. Y., Tse, H. F., Lau, C. P., and Li, G. R. (2010). Multiple Ca²⁺ signaling pathways regulate intracellular Ca²⁺ activity in human cardiac fibroblasts. *J. Cell. Physiol.* 223 (1), 68–75. doi:10.1002/jcp.22010
- Chen, X., Egly, C., Riley, A. M., Li, W., Tewson, P., Hughes, T. E., et al. (2014). PKC-dependent phosphorylation of the H₁ histamine receptor modulates TRPC6 activity. *Cells* 3 (2), 247–257. doi:10.3390/cells3020247
- Chung, C. C., Chen, P. H., Lin, Y. F., Kao, Y. H., and Chen, Y. J. (2021). Lithium reduces migration and collagen synthesis activity in human cardiac fibroblasts by inhibiting store-operated Ca²⁺ entry. *Int. J. Mol. Sci.* 22 (2), E842. doi:10.3390/ijms22020842
- Clapham, D. E. (2007). Calcium signaling. *Cell* 131 (6), 1047–1058. doi:10.1016/j.cell.2007.11.028
- Dharmage, S. C., Perret, J. L., and Custovic, A. (2019). Epidemiology of asthma in children and adults. *Front. Pediatr.* 7, 246. doi:10.3389/fped.2019.00246
- Dragoni, S., Laforenza, U., Bonetti, E., Lodola, F., Bottino, C., Berra-Romani, R., et al. (2011). Vascular endothelial growth factor stimulates endothelial colony forming cells proliferation and tubulogenesis by inducing oscillations in intracellular Ca²⁺ concentration. *Stem Cells* 29 (11), 1898–1907. doi:10.1002/stem.734
- Dupont, G., and Combettes, L. (2016). *Fine tuning of cytosolic Ca (2+) oscillations*, 5, F1000Res. doi:10.12688/f1000research.8438.1Review
- Dupont, G., and Croisier, H. (2010). Spatiotemporal organization of Ca²⁺ dynamics: A modeling-based approach. *HFSP J.* 4 (2), 43–51. doi:10.2976/1.3385660
- Dupont, G. (2014). Modeling the intracellular organization of calcium signaling. *Wiley Interdiscip. Rev. Syst. Biol. Med.* 6 (3), 227–237. doi:10.1002/wsbm.1261
- Emrich, S. M., Yoast, R. E., Xin, P., Arige, V., Wagner, L. E., Hempel, N., et al. (2021). Omnitemporal choreographies of all five STIM/Orai and IP₃Rs underlie the complexity of mammalian Ca²⁺ signaling. *Cell Rep.* 34 (9), 108760. doi:10.1016/j.celrep.2021.108760
- Espinosa-Tanguma, R., O'Neil, C., Chrones, T., Pickering, J. G., and Sims, S. M. (2011). Essential role for calcium waves in migration of human vascular smooth muscle cells. *Am. J. Physiol. Heart Circ. Physiol.* 301 (2), H315–H323. doi:10.1152/ajpheart.00355.2010
- Faris, P., Casali, C., Negri, S., Jengo, L., Biggiogera, M., Maione, A. S., et al. (2022). Nicotinic acid adenine dinucleotide phosphate induces intracellular Ca²⁺ signalling and stimulates proliferation in human cardiac mesenchymal stromal cells. *Front. Cell Dev. Biol.* 10, 874043. doi:10.3389/fcell.2022.874043
- Ferrera, L., Barbieri, R., Picco, C., Zuccolini, P., Remigante, A., Bertelli, S., et al. (2021). TRPM2 oxidation activates two distinct potassium channels in melanoma cells through intracellular calcium increase. *Int. J. Mol. Sci.* 22 (16), 8359. doi:10.3390/ijms22168359
- Gambardella, J., Morelli, M. B., Wang, X., Castellanos, V., Mone, P., and Santulli, G. (2021). The discovery and development of IP₃ receptor modulators: An update. *Expert Opin. Drug Discov.* 16 (6), 709–718. doi:10.1080/17460441.2021.1858792
- Garbuzenko, E., Berkman, N., Puxeddu, I., Kramer, M., Nagler, A., and Levi-Schaffer, F. (2004). Mast cells induce activation of human lung fibroblasts *in vitro*. *Exp. Lung Res.* 30 (8), 705–721. doi:10.1080/01902140490517809
- GBD Diseases and Injuries Collaborators (2020). Global burden of 369 diseases and injuries in 204 countries and territories, 1990–2019: A systematic analysis for the global burden of disease study 2019. *Lancet* 396 (10258), 1204–1222. doi:10.1016/S0140-6736(20)30925-9
- Gutiérrez-Venegas, G., and Rodríguez-Pérez, C. E. (2012). Toll-like receptor 3 activation promotes desensitization of histamine response in human gingival fibroblasts: Poly (I:C) induces histamine receptor desensitization in human gingival fibroblasts. *Cell. Immunol.* 273 (2), 150–157. doi:10.1016/j.cellimm.2011.12.005
- Guzmán-Silva, A., Vázquez de Lara, L. G., Torres-Jácome, J., Vargaz-Guadarrama, A., Flores-Flores, M., Pezzat Said, E., et al. (2015). Lung beractant increases free cytosolic levels of Ca²⁺ in human lung fibroblasts. *PLoS One* 10 (7), e0134564. doi:10.1371/journal.pone.0134564
- Haas, H. L., Sergeeva, O. A., and Selbach, O. (2008). Histamine in the nervous system. *Physiol. Rev.* 88 (3), 1183–1241. doi:10.1152/physrev.00043.2007
- Hobai, I. A., Hancox, J. C., and Levi, A. J. (2000). Inhibition by nickel of the L-type Ca channel in Guinea pig ventricular myocytes and effect of internal cAMP. *Am. J. Physiol. Heart Circ. Physiol.* 279 (2), H692–H701. doi:10.1152/ajpheart.2000.279.2.H692
- Hofmann, K., Fiedler, S., Vierkotten, S., Weber, J., Klee, S., Jia, J., et al. (2017). Classical transient receptor potential 6 (TRPC6) channels support myofibroblast differentiation and development of experimental pulmonary fibrosis. *Biochim. Biophys. Acta. Mol. Basis Dis.* 1863 (2), 560–568. doi:10.1016/j.bbdis.2016.12.002
- Horie, M., Saito, A., Yamauchi, Y., Mikami, Y., Sakamoto, M., Jo, T., et al. (2014). Histamine induces human lung fibroblast-mediated collagen gel contraction via histamine H1 receptor. *Exp. Lung Res.* 40 (5), 222–236. doi:10.3109/01902148.2014.900155
- Ikawa, Y., Shiba, K., Ohki, E., Mutoh, N., Suzuki, M., Sato, H., et al. (2008). Comparative study of histamine H4 receptor expression in human dermal fibroblasts. *J. Toxicol. Sci.* 33 (4), 503–508. doi:10.2131/jts.33.503
- Ishida, S., Matsu-Ura, T., Fukami, K., Michikawa, T., and Mikoshiba, K. (2014). Phospholipase C-β1 and β4 contribute to non-genetic cell-to-cell variability in histamine-induced calcium signals in HeLa cells. *PLoS One* 9 (1), e86410. doi:10.1371/journal.pone.0086410
- Janssen, L. J., Mukherjee, S., and Ask, K. (2015). Calcium homeostasis and ionic mechanisms in pulmonary fibroblasts. *Am. J. Respir. Cell Mol. Biol.* 53 (2), 135–148. doi:10.1165/rcmb.2014-0269TR
- Jing, D., Lu, X. L., Luo, E., Sajda, P., Leong, P. L., and Guo, X. E. (2013). Spatiotemporal properties of intracellular calcium signaling in osteocytic and osteoblastic cell networks under fluid flow. *Bone* 53 (2), 531–540. doi:10.1016/j.bone.2013.01.008
- Johnson, C. M., Johnson, C., Bazan, E., Garver, D., Gruenstein, E., and Ahluwalia, M. (1990). Histamine receptors in human fibroblasts: Inositol phosphates, Ca²⁺, and cell growth. *Am. J. Physiol.* 258 (1), C533–C543. doi:10.1152/ajpcell.1990.258.3.C533
- Johnson, M. T., Xin, P., Benson, J. C., Pathak, T., Walter, V., Emrich, S. M., et al. (2022). STIM1 is a core trigger of airway smooth muscle remodeling and hyperresponsiveness in asthma. *Proc. Natl. Acad. Sci. U. S. A.* 119 (1), e2114557118. doi:10.1073/pnas.2114557118
- Jordana, M., Befus, A. D., Newhouse, M. T., Bienenstock, J., and Gauldie, J. (1988). Effect of histamine on proliferation of normal human adult lung fibroblasts. *Thorax* 43 (7), 552–558. doi:10.1136/thx.43.7.552
- Kemény, L. V., Schnúr, A., Czepán, M., Rakonczay, Z., Gál, E., Lonovics, J., et al. (2013). Na⁺/Ca²⁺ exchangers regulate the migration and proliferation of human gastric myofibroblasts. *Am. J. Physiol. Gastrointest. Liver Physiol.* 305 (8), G552–G563. doi:10.1152/ajpgi.00394.2012
- Kohyama, T., Yamauchi, Y., Takizawa, H., Kamitani, S., Kawasaki, S., and Nagase, T. (2010). Histamine stimulates human lung fibroblast migration. *Mol. Cell. Biochem.* 337 (1–2), 77–81. doi:10.1007/s11010-009-0287-y
- Kunzmann, S., Schmidt-Weber, C., Zingg, J. M., Azzi, A., Kramer, B. W., Blaser, K., et al. (2007). Connective tissue growth factor expression is regulated by histamine in lung fibroblasts: Potential role of histamine in airway remodeling. *J. Allergy Clin. Immunol.* 119 (6), 1398–1407. doi:10.1016/j.jaci.2007.02.018
- Lembong, J., Sabass, B., Sun, B., Rogers, M. E., and Stone, H. A. (2015). Mechanics regulates ATP-stimulated collective calcium response in fibroblast cells. *J. R. Soc. Interface* 12 (108), 20150140. doi:10.1098/rsif.2015.0140
- Leurs, R., Smit, M. J., Bast, A., and Timmerman, H. (1990). Different profiles of desensitization dynamics in Guinea-pig jejunal longitudinal smooth muscle after stimulation with histamine and methacholine. *Br. J. Pharmacol.* 101 (4), 881–888. doi:10.1111/j.1476-5381.1990.tb14175.x
- Leurs, R., Smit, M. J., Bast, A., and Timmerman, H. (1991). Homologous histamine H1 receptor desensitization results in reduction of H1 receptor agonist efficacy. *Eur. J. Pharmacol.* 196 (3), 319–322. doi:10.1016/0014-2999(91)90446-w
- Liang, W., McDonald, P., McManus, B., van Breemen, C., and Wang, X. (2003). Histamine-induced Ca(2+) signaling in human valvular myofibroblasts. *J. Mol. Cell. Cardiol.* 35 (4), 379–388. doi:10.1016/s0022-2828(03)00010-5
- Maini, R., Collison, D. J., Maidment, J. M., Davies, P. D., and Wormstone, I. M. (2002). Pterygial derived fibroblasts express functionally active histamine and epidermal growth factor receptors. *Exp. Eye Res.* 74 (2), 237–244. doi:10.1006/exer.2001.1116

- Moccia, F., Berra-Romani, R., Tritto, S., Signorelli, S., Taglietti, V., and Tanzi, F. (2003). Epidermal growth factor induces intracellular Ca²⁺ oscillations in microvascular endothelial cells. *J. Cell. Physiol.* 194 (2), 139–150. doi:10.1002/jcp.10198
- Moccia, F., Nusco, G. A., Lim, D., Kyozuka, K., and Santella, L. (2006). NAADP and InsP3 play distinct roles at fertilization in starfish oocytes. *Dev. Biol.* 294 (1), 24–38. doi:10.1016/j.ydbio.2006.02.011
- Moccia, F., Zuccolo, E., Poletto, V., Turin, I., Guerra, G., Pedrazzoli, P., et al. (2016). Targeting Stim and Orai proteins as an alternative approach in anticancer therapy. *Curr. Med. Chem.* 23 (30), 3450–3480. doi:10.2174/0929867323666160607111220
- Mukherjee, S., Ayaub, E. A., Murphy, J., Lu, C., Kolb, M., Ask, K., et al. (2015). Disruption of calcium signaling in fibroblasts and attenuation of bleomycin-induced fibrosis by nifedipine. *Am. J. Respir. Cell Mol. Biol.* 53 (4), 450–458. doi:10.1165/rcmb.2015-0009OC
- Murdoch, J. R., and Lloyd, C. M. (2010). Chronic inflammation and asthma. *Mutat. Res.* 690 (1–2), 24–39. doi:10.1016/j.mrfmmm.2009.09.005
- Negri, S., Faris, P., Berra-Romani, R., Guerra, G., and Moccia, F. (2019). Endothelial transient receptor potential channels and vascular remodeling: Extracellular Ca²⁺ entry for angiogenesis, arteriogenesis and vasculogenesis. *Front. Physiol.* 10, 1618. doi:10.3389/fphys.2019.01618
- Negri, S., Faris, P., Maniezi, C., Pellavio, G., Spaiardi, P., Botta, L., et al. (2021). NMDA receptors elicit flux-independent intracellular Ca²⁺ signals via metabotropic glutamate receptors and flux-dependent nitric oxide release in human brain microvascular endothelial cells. *Cell Calcium* 99, 102454. doi:10.1016/j.ceca.2021.102454
- Niisato, N., Ogata, Y., Furuyama, S., and Sugiyama, H. (1996). Histamine H1 receptor-induced Ca²⁺ mobilization and prostaglandin E2 release in human gingival fibroblasts. Possible role of receptor-operated Ca²⁺ influx. *Biochem. Pharmacol.* 52 (7), 1015–1023. doi:10.1016/0006-2952(96)00417-0
- Ogata, Y., Nakao, S., Suzuki, T., Tsunoda, S., Furuyama, S., and Sugiyama, H. (1999). Involvement of prostaglandins in histamine H1 receptor-operated Ca²⁺ entry in human gingival fibroblasts. *Life Sci.* 64 (4), P171–7. doi:10.1016/s0024-3205(98)00565-7
- Okumura, W., Kozono, T., Sato, H., Matsui, H., Takagi, T., Tonozuka, T., et al. (2022). Jaw1/LRMP increases Ca²⁺ influx upon GPCR stimulation with heterogeneous effect on the activity of each ITPR subtype. *Sci. Rep.* 12 (1), 9476. doi:10.1038/s41598-022-13620-4
- Ong, H. L., Subedi, K. P., Son, G. Y., Liu, X., and Ambudkar, I. S. (2019). Tuning store-operated calcium entry to modulate Ca²⁺-dependent physiological processes. *Biochim. Biophys. Acta. Mol. Cell Res.* 1866 (7), 1037–1045. doi:10.1016/j.bbamer.2018.11.018
- Paltauf-Doburzynska, J., Frieden, M., Spitaler, M., and Graier, W. F. (2000). Histamine-induced Ca²⁺ oscillations in a human endothelial cell line depend on transmembrane ion flux, ryanodine receptors and endoplasmic reticulum Ca²⁺-ATPase. *J. Physiol.* 524 (3), 701–713. doi:10.1111/j.1469-7793.2000.00701.x
- Panula, P., Chazot, P. L., Cowart, M., Gutzmer, R., Leurs, R., Liu, W. L., et al. (2015). International union of basic and clinical pharmacology. XCIX. Angiotensin receptors: Interpreters of pathophysiological angiotensinergic stimuli [corrected]. *Pharmacol. Rev.* 67 (3), 601–655. doi:10.1124/pr.114.010249
- Panula, P. (2021). Histamine receptors, agonists, and antagonists in health and disease. *Handb. Clin. Neurol.* 180, 377–387. doi:10.1016/b978-0-12-820107-7.00023-9
- Parker, I., and Ivorra, I. (1991). Caffeine inhibits inositol trisphosphate-mediated liberation of intracellular calcium in *Xenopus* oocytes. *J. Physiol.* 433, 229–240. doi:10.1113/jphysiol.1991.sp018423
- Peppiatt, C. M., Collins, T. J., Mackenzie, L., Conway, S. J., Holmes, A. B., Bootman, M. D., et al. (2003). 2-Aminoethoxydiphenyl borate (2-APB) antagonises inositol 1, 4, 5-trisphosphate-induced calcium release, inhibits calcium pumps and has a use-dependent and slowly reversible action on store-operated calcium entry channels. *Cell Calcium* 34 (1), 97–108. doi:10.1016/s0143-4160(03)00026-5
- Pinheiro, A. R., Paramos-de-Carvalho, D., Certal, M., Costa, M. A., Costa, C., Magalhães-Cardoso, M. T., et al. (2013). Histamine induces ATP release from human subcutaneous fibroblasts, via pannexin-1 hemichannels, leading to Ca²⁺ mobilization and cell proliferation. *J. Biol. Chem.* 288 (38), 27571–27583. doi:10.1074/jbc.M113.460865
- Prakriya, M., and Lewis, R. S. (2015). Store-operated calcium channels. *Physiol. Rev.* 95 (4), 1383–1436. doi:10.1152/physrev.00020.2014
- Pulina, M. V., Zulian, A., Berra-Romani, R., Beskina, O., Mazzocco-Spezia, A., Baryshnikov, S. G., et al. (2010). Upregulation of Na⁺ and Ca²⁺ transporters in arterial smooth muscle from ouabain-induced hypertensive rats. *Am. J. Physiol. Heart Circ. Physiol.* 298 (1), H263–H274. doi:10.1152/ajpheart.00784.2009
- Rahman, M., Mukherjee, S., Sheng, W., Nilus, B., and Janssen, L. J. (2016). Electrophysiological characterization of voltage-dependent calcium currents and TRPV4 currents in human pulmonary fibroblasts. *Am. J. Physiol. Lung Cell. Mol. Physiol.* 310 (7), L603–L614. doi:10.1152/ajplung.00426.2015
- Remigante, A., Zuccolini, P., Barbieri, R., Ferrera, L., Morabito, R., Gavazzo, P., et al. (2021). NS-11021 modulates cancer-associated processes independently of BK channels in melanoma and pancreatic duct adenocarcinoma cell lines. *Cancers (Basel)* 13 (23), 6144. doi:10.3390/cancers13236144
- Sadras, F., Monteith, G. R., and Roberts-Thomson, S. J. (2021a). An emerging role for calcium signaling in cancer-associated fibroblasts. *Int. J. Mol. Sci.* 22 (21), 11366. doi:10.3390/ijms222111366
- Sadras, F., Stewart, T. A., Robitaille, M., Peters, A. A., Croft, P. K., Soon, P. S., et al. (2021b). Altered calcium influx pathways in cancer-associated fibroblasts. *Biomedicines* 9 (6), 680. doi:10.3390/biomedicines9060680
- Saliba, Y., Karam, R., Smayra, V., Aftimos, G., Abramowitz, J., Birnbaumer, L., et al. (2015). Evidence of a role for fibroblast transient receptor potential canonical 3 Ca²⁺ channel in renal fibrosis. *J. Am. Soc. Nephrol.* 26 (8), 1855–1876. doi:10.1681/ASN.2014010065
- Salomonsson, M., Malinowski, A., Kalm-Stephens, P., Dahlin, J. S., Janson, C., Alving, K., et al. (2019). Circulating mast cell progenitors correlate with reduced lung function in allergic asthma. *Clin. Exp. Allergy* 49 (6), 874–882. doi:10.1111/cea.13388
- Sanchez-Collado, J., Lopez, J. J., Gonzalez-Gutierrez, L., Cantonero, C., Jardin, I., Salido, G. M., et al. (2020). Functional role of TRPC6 and STIM2 in cytosolic and endoplasmic reticulum Ca²⁺ content in resting estrogen receptor-positive breast cancer cells. *Biochem. J.* 477 (17), 3183–3197. doi:10.1042/BCJ20200560
- Santella, L. (1998). The role of calcium in the cell cycle: Facts and hypotheses. *Biochem. Biophys. Res. Commun.* 244 (2), 317–324. doi:10.1006/bbrc.1998.8086
- Sarasola, M. P., Táquez Delgado, M. A., Nicoud, M. B., and Medina, V. A. (2021). Histamine in cancer immunology and immunotherapy. Current status and new perspectives. *Pharmacol. Res. Perspect.* 9 (5), e00778. doi:10.1002/prp2.778
- Sauvé, R., Diarra, A., Chahine, M., Simoneau, C., Morier, N., and Roy, G. (1991). Ca²⁺ oscillations induced by histamine H1 receptor stimulation in HeLa cells: Fura-2 and patch clamp analysis. *Cell Calcium* 12 (2–3), 165–176. doi:10.1016/0143-4160(91)90018-a
- Seifert, R., Strasser, A., Schneider, E. H., Neumann, D., Dove, S., and Buschauer, A. (2013). Molecular and cellular analysis of human histamine receptor subtypes. *Trends Pharmacol. Sci.* 34 (1), 33–58. doi:10.1016/j.tips.2012.11.001
- Smedler, E., and Uhlén, P. (2014). Frequency decoding of calcium oscillations. *Biochim. Biophys. Acta* 1840 (3), 964–969. doi:10.1016/j.bbagen.2013.11.015
- Smit, M. J., Bloemers, S. M., Leurs, R., Tertoolen, L. G., Bast, A., de Laat, S. W., et al. (1992). Short-term desensitization of the histamine H1 receptor in human HeLa cells: Involvement of protein kinase C dependent and independent pathways. *Br. J. Pharmacol.* 107 (2), 448–455. doi:10.1111/j.1476-5381.1992.tb12766.x
- Soulsby, M. D., and Wojcikiewicz, R. J. (2002). 2-Aminoethoxydiphenyl borate inhibits inositol 1, 4, 5-trisphosphate receptor function, ubiquitination and downregulation, but acts with variable characteristics in different cell types. *Cell Calcium* 32 (4), 175–181. doi:10.1016/s0143416002001525
- Tomioka, M., Ida, S., Shindoh, Y., Ishihara, T., and Takishima, T. (1984). Mast cells in bronchoalveolar lumen of patients with bronchial asthma. *Am. Rev. Respir. Dis.* 129 (6), 1000–1005. doi:10.1164/arrd.1984.129.6.1000
- Vazquez-de-Lara, L. G., Tlatelpa-Romero, B., Romero, Y., Fernández-Tamayo, N., Vazquez-de-Lara, F., M Justo-Janeiro, J., et al. (2018). Phosphatidylethanolamine induces an antifibrotic phenotype in normal human lung fibroblasts and ameliorates bleomycin-induced lung fibrosis in mice. *Int. J. Mol. Sci.* 19 (9), E2758. doi:10.3390/ijms19092758
- Veerappan, A., O'Connor, N. J., Brazin, J., Reid, A. C., Jung, A., McGee, D., et al. (2013). Mast cells: A pivotal role in pulmonary fibrosis. *DNA Cell Biol.* 32 (4), 206–218. doi:10.1089/dna.2013.2005
- Wacquier, B., Voorsluys, V., Combettes, L., and Dupont, G. (2019). Coding and decoding of oscillatory Ca²⁺ signals. *Semin. Cell Dev. Biol.* 94, 11–19. doi:10.1016/j.semcdb.2019.01.008
- Wilson, C., Zhang, X., Lee, M. D., MacDonald, M., Heathcote, H. R., Alorfi, N. M. N., et al. (2020). Disrupted endothelial cell heterogeneity and network organization impair vascular function in prediabetic obesity. *Metabolism.* 111, 154340. doi:10.1016/j.metabol.2020.154340
- Wu, C. Y., Hsu, W. L., Tsai, M. H., Chai, C. Y., Yen, C. J., Chen, C. H., et al. (2019). A potential new approach for treating systemic sclerosis: Dedifferentiation of SSC fibroblasts and change in the microenvironment by blocking store-operated Ca²⁺ entry. *PLoS One* 14 (3), e0213400. doi:10.1371/journal.pone.0213400
- Yamauchi, K., and Ogasawara, M. (2019). The role of histamine in the pathophysiology of asthma and the clinical efficacy of antihistamines in asthma therapy. *Int. J. Mol. Sci.* 20 (7), E1733. doi:10.3390/ijms20071733

- Yoast, R. E., Emrich, S. M., Zhang, X., Xin, P., Johnson, M. T., Fike, A. J., et al. (2020). The native ORAI channel trio underlies the diversity of Ca^{2+} signaling events. *Nat. Commun.* 11 (1), 2444. doi:10.1038/s41467-020-16232-6
- Zenmyo, M., Hiraoka, K., Komiya, S., Morimatsu, M., and Sasaguri, Y. (1995). Histamine-stimulated production of matrix metalloproteinase 1 by human rheumatoid synovial fibroblasts is mediated by histamine H1-receptors. *Virchows Arch.* 427 (4), 437–444. doi:10.1007/bf00199394
- Zhang, J., Berra-Romani, R., Sinnegger-Brauns, M. J., Striessnig, J., Blaustein, M. P., and Matteson, D. R. (2007). Role of Cav1.2 L-type Ca^{2+} channels in vascular tone: Effects of nifedipine and Mg^{2+} . *Am. J. Physiol. Heart Circ. Physiol.* 292 (1), H415–H425. doi:10.1152/ajpheart.01214.2005
- Zhang, X., Xin, P., Yoast, R. E., Emrich, S. M., Johnson, M. T., Pathak, T., et al. (2020). Distinct pharmacological profiles of ORAI1, ORAI2, and ORAI3 channels. *Cell Calcium* 91, 102281. doi:10.1016/j.ceca.2020.102281
- Zheng, T., Nathanson, M. H., and Elias, J. A. (1994). Histamine augments cytokine-stimulated IL-11 production by human lung fibroblasts. *J. Immunol.* 153 (10), 4742–4752.
- Zuccolini, P., Ferrera, L., Remigante, A., Picco, C., Barbieri, R., Bertelli, S., et al. (2022). The VRAC blocker DCPIB directly gates the BK channels and increases intracellular Ca^{2+} in melanoma and pancreatic duct adenocarcinoma cell lines. *Br. J. Pharmacol.* 179 (13), 3452–3469. doi:10.1111/bph.15810
- Zuccolo, E., Laforenza, U., Ferulli, F., Pellavio, G., Scarpellino, G., Tanzi, M., et al. (2018). Stim and Orai mediate constitutive Ca^{2+} entry and control endoplasmic reticulum Ca^{2+} refilling in primary cultures of colorectal carcinoma cells. *Oncotarget* 9 (57), 31098–31119. doi:10.18632/oncotarget.25785
- Zuccolo, E., Laforenza, U., Negri, S., Botta, L., Berra-Romani, R., Faris, P., et al. (2019). Muscarinic M5 receptors trigger acetylcholine-induced Ca^{2+} signals and nitric oxide release in human brain microvascular endothelial cells. *J. Cell. Physiol.* 234 (4), 4540–4562. doi:10.1002/jcp.27234